الجمهورية الجزائرية الديمقراطية الشعبية
People's Democratic Republic of Algeria
وزارة التعليم العالي والبحث العلمي
Ministry of Height Education and Scientific research

University of Ghardaïa
Faculty of Sciences and Technology
Department of Common Teaching in Sciences and Technology

جامعة غرداية
كلية العلوم والتكنولوجيا
قسم التعليم المشترك في العلوم والتكنولوجيا

Approval for Final Printing of a Master's Dissertation

	Name and Surname	Signature
Examiner 1	Cherif Salah	
Examiner 2	BOUDABIA SAAD	
Supervisor	Azzaoui Mohammed	

I, the undersigned, Mr: ..... Boudabia Saad

President of the jury for the student(s): ..... Bekkaye Khira .....

Field: Physics; **Specialization:** Energy physics

Thesis Title: ..... Optical and thermal study of a solar radiation concentrator for laser production

Hereby authorize the above-mentioned student(s) to print and submit their final manuscript to the department.

Ghardaia : 19../ 04../ 2016

President of the jury

Head of the department

جامعة غرداية
قسم التعليم المشترك في العلوم والتكنولوجيا
كلية العلوم و التكنولوجيا

رئيس قسم التعليم المشترك في العلوم والتكنولوجيا
ثنوية فيصل

الجمهورية الجزائرية الديمقراطية الشعبية
People's Democratic Republic of Algeria
وزارة التعليم العالي والبحث العلمي
Ministry of Higher Education and Scientific Research
جامعة غرداية
University of Ghardaia

N° Registration

كلية العلوم والتكنولوجيا
Faculty of Science and Technology
قسم التعليم المشترك في العلوم و التكنولوجيا
Department of common Teaching in sciences and technology

Thesis

For obtaining the master's degree

Master

Field: Material Sciences

Sector: Physics

Speciality: Energy Physics and Renewable Energies

Thesis

Optical and thermal study of a solar radiation concentrator for laser production

Presented by: BEKKAYE Khira

publicly defended on ……../……/……..

In front of the jury composed of:

BOUDABIA Saad	**MCA**	**Univ Ghardaia**	**President**
AZZAOUI Mohammed	**MCB**	**Univ Ghardaia**	**Supervisor**
CHERIF Salah	**MCB**	**Univ Ghardaia**	**Examiner**

Academic year :2024/2025

Thanks

I would like to express my sincere gratitude and appreciation to everyone who contributed to the completion of this thesis.

My deepest thanks go to my supervisor

Dr. AZZAOUI Mohammed,

for his valuable scientific guidance, patience, and continuous encouragement throughout the entire duration of this work.

I would also like to extend my sincere thanks to all the professors of

The Department of Common Core in Science and Technology at the University of Ghardaia,

for the knowledge and education, they have provided us over the years especially

Dr. CHOUIA Fayçal,

whom I gratefully acknowledge.

My heartfelt gratitude goes to my dear family, who have always been a source of support and moral strength throughout every stage of my academic journey, and to everyone who stood by me and offered encouragement even with just a kind word.

To my colleagues and friends who shared this academic journey with me, I say:

Thank you for every moment of cooperation and shared effort.

Dedication

In the name of Allah, the most compassionate. This humble effort is dedicated

TO MY DIVINLY PARENTS

I dedicate this memory to my loved parents who have always teach me to trust in Allah, believe in hard work and teach me that so much could be done with little.

TO MY RESPECTED TEACHERS

Teachers are always great source of inspiration and motivation to me. However, my teacher's remained beacon of light for me.

Their sincere guidance and prudent leadership guided my way clearly not only to excel in achieving this dissertation but also definite direction for professional career too.

TO MY SWEET FRIENDS

My friends mean world to me. I am proud to say that save their cooperation, collaboration and team work, I would not be able to achieve this target easily. I'm more than thankful to all for their support and encouragement during the time, I need them most...

الملخص

هذا العمل يقدم محاكاة لنظام تركيز الطاقة الشمسية في منطقة غرداية بالجزائر، باستخدام أطباق مكافئة بأقطار مختلفة. اعتمدت الدراسة على الإحداثيات الجغرافية للمنطقة: خط الطول 3.6833°، خط العرض 32.483°، والارتفاع 450 متر فوق مستوى سطح البحر. يركز النظام الإشعاع الشمسي نحو ليزر صلب من نوعNd:YAG ، وتم تحليله تحت حالتين: بدون و مع مرشح طيفي للأشعة تحت الحمراء.

تم تقييم الأداء من حيث الإشعاع الشمسي، الطاقة المجمعة، وخرج الليزر. بلغ الإشعاع الشمسي أقصى قيمة حوالي 850 واط/م² عند منتصف النهار، مع شدة بؤرية تصل إلى 10,500 واط/م² بدون الترشيح و5,300 واط/م² مع الترشيح. بلغت القدرة المجمعة القصوى للصحن حوالي 8,800 واط، وتنخفض إلى 4,500 واط عند استخدام المرشح، بينما وصل خرج الليزر إلى حوالي 52 واط.

تؤكد هذه النتائج فعالية الأطباق المكافئة في تركيز الطاقة الشمسية، وتوضح جدوى أنظمة الليزر المضخ بالطاقة الشمسية، خصوصًا في المناطق ذات الإشعاع الشمسي العالي. كما تسلط الضوء على اعتماد الأداء على المعايير البصرية والهندسية مثل قطر الصحن والطول البؤري.

الكلمات المفتاحية :الإشعاع الشمسي، مركز شمسي، ليزر، Nd:YAG، الطاقة الشمسية، القدرة الخارجة.

Abstract

This work presents a simulation of a solar concentrating system in the Ghardaia region of Algeria, using parabolic dishes of varying diameters. The study employed the region's geographical coordinates: longitude 3.6833°, latitude 32.483°, and altitude 450 m above sea level. The system concentrates solar radiation onto a solid-state Nd:YAG laser and was analyzed under two conditions: without and with an infrared microfilter.

The performance was evaluated in terms of solar irradiance, collected energy, and laser output. Solar irradiance reached a maximum of approximately 850 W/m² around noon, with focal irradiance up to 10,500 W/m² without filtering and 5,300 W/m² with the filter. The total power collected by the dish peaked at about 8,800 W, decreasing to 4,500 W with filtering, while the laser output reached a maximum of approximately 52 W.

These results confirm the effectiveness of parabolic dish concentrators in focusing solar energy and demonstrate the feasibility of solar-pumped laser systems, particularly in high solar radiation regions. They also highlight the dependence of performance on optical and geometrical parameters, such as dish diameter and focal length.

Keywords: solar radiation, solar concentrator, laser, Nd:YAG, solar energy, output power.

Résumé

Ce travail présente une simulation d'un système de concentration solaire dans la région de Ghardaïa, en Algérie, utilisant des plats paraboliques de diamètres variés. L'étude s'est basée sur les coordonnées géographiques de la région : longitude 3,6833°, latitude 32,483° et altitude 450 m au-dessus du niveau de la mer. Le système concentre le rayonnement solaire sur un laser à état solide Nd:YAG et a été analysé dans deux conditions : sans et avec un microfiltre infrarouge.

La performance a été évaluée en termes d'irradiance solaire, d'énergie collectée et de puissance de sortie du laser. L'irradiance solaire a atteint un maximum d'environ 850 W/m² vers midi, avec une irradiance focale jusqu'à 10 500 W/m² sans filtrage et 5 300 W/m² avec filtrage. La puissance totale collectée par le plat a culminé à environ 8 800 W, diminuant à 4 500 W avec le filtre, tandis que la puissance de sortie du laser a atteint environ 52 W.

Ces résultats confirment l'efficacité des plats paraboliques pour concentrer l'énergie solaire et démontrent la faisabilité des systèmes de lasers pompés par l'énergie solaire, en particulier dans les régions à fort rayonnement solaire. Ils mettent également en évidence la dépendance de la performance aux paramètres optiques et géométriques, tels que le diamètre du plat et la longueur focale.

Mots-clés : rayonnement solaire, concentrateur solaire, laser, Nd:YAG, énergie solaire, puissance de sortie.

List of Contents

List of figures

List of tables

List of Symbols

Symbol	Physical Quantity	Unit
N	the wave frequency	Hz
λ	the wavelength	m
C	the speed of light in vacuum	m/s
H	the plank constant	J.s
G_{so}	Solar constant	W/m²
N	the number is the day of the year	/
h_s	Solar altitude angle	Degrees (°)
TST	True solar time	min
MST	Mean solar time	min
Z	altitude of the location above sea level, expressed	km
AM	optical air mass	/
I	Direct solar irradiance	W/m²
A	Area	m²
a	Solar azimuth angle	Degrees (°)
f_a	Geometric view factor	m
f_c	Friction coefficient	/
c_g	Solar gain	/
c_p	Specific heat capacity	J/(kg·K)
D	Diameter	m
E	the energy of the photon	J
Et	Equation of time	min
N	the population of the energy level	/
Γ	optical gain coefficient	/
α	total intracavity loss coefficient (excluding output coupling)	/
L	length of the optical cavity	m
A_α	The cross-sectional area of the rod.	m ²
I_s	The saturation flux.	W/m²
η_q	The quantum efficiency.	/
η_{ovp}	The overlap ratio.	/
ε	The pumping efficiency.	/

Θ	Angle of incidence (solar radiation incident angle)	Degrees (°)
δ	the angle formed by the direction of the sun whith its projection on the equatorial plane	Degrees (°)
Ω	Hour angle	Degrees (°)

General Introduction

General introduction

The use of renewable energy is increasing worldwide. This use may hold the key to combating climate change and contribute to reducing pollution, as well as being a reliable source of energy.

Renewable energy uses energy sources that are continually replenished by nature, such as the sun, wind, water, the Earth's heat, and plants. Renewable energy technologies convert these resources into usable forms of energy, most often electricity, but also heat, chemicals, or mechanical power [1].

Solar energy is the largest inexhaustible source of energy. Almost all countries in the world receive solar energy.

The sun is considered one of the most important sources of renewable energy, as it emits an enormous amount of energy with a power density of approximately 63 kw/m². The Earth receives about 1.7×10^{17} watts of this energy, with a power density of around 1 kw/m² on the Earth's surface which is approximately 10000 times the global for energy therefore this energy exported in various fields [2 ,3,7].

Solar radiation is exploited in several fields, such as optoelectronics, energy production, agriculture, medicine, industry, space technologies, and environmental applications.

Among the most interesting human discoveries in this field is the laser, particularly the solar laser.

The geographical location of the Ghardaia region in Algeria is characterized by high number of sunshine hours.

It is also characterized by low rainfall, which makes it suitable for thermal and optical studies. We conducted a thermal and optical study to obtain a relatively high laser collection efficiency based on the intensity of solar radiation.

The solar concentrator used is a parabolic dish with different diameters, without resorting to solar tracking, which makes the system simple.

We also used a side pump for the active materials in order to produce a solar laser. To avoid a rise in temperature at the level of the active material, a cooling system and a spectral filter were added to protect it from damage.

We will divide this study into three chapters:

The first chapter will be titled "Solar Radiation and Solar Concentrators." In it, we will discuss the concept of solar radiation, the factors affecting its distribution, as well as solar angles, and temporal, horizontal, and terrestrial coordinates. We will then move on to equations for estimating solar radiation and types of solar tracking. Next, we will explore the different types of solar concentrators, with a particular focus on the parabolic dish. A photometric study of the parabolic dish and its luminous output will also be conducted.

General Introduction

The second chapter will be titled "Lasers and Solar Lasers." We will explain the concept of lasers and their components, followed by their working principle. This will include the processes of absorption, spontaneous emission, stimulated emission, optical amplification, and both three-level and four-level laser systems, along with the various types of lasers. Afterward, we will delve into the concept and technology of solar lasers, their pumping methods, and finally, we will conclude the chapter with a discussion on laser efficiency and a summary.

The third chapter will be titled "Numerical Study, Analysis, and Discussion of Results." In this chapter, we will carry out a numerical study of the model and present the expected results. We will analyse the concentrated solar radiation obtained, and compare the energy and power output with and without a solar spectrum filter. The output power of the Nd:YAG laser will also be evaluated, discussed, and interpreted.

Finally, we have summarized the results in a general conclusion and future prospects.

Chapter 01:

Solar radiation and solar concentrators

Chapter 1: Solar radiation and solar concentrators

1.1. Introduction

Solar energy is the fundamental source of almost all energy forms on Earth, including both fossil fuels and renewable energy. It is abundant, widely distributed, easy to use, and economically viable. Since ancient times, humans have exploited solar energy to satisfy their basic needs. With the progress of industry and technology, the use of solar energy has significantly evolved.

Solar energy can be harnessed primarily through two processes: thermal conversion**,** which involves heating fluids by exposing them to solar radiation and photovoltaic conversion, where solar cells convert sunlight directly into electrical energy.

1.2. Sun and solar radiation energy

1.2.1 Sun

The Sun is the central star of our solar system. It consists mainly of hydrogen and helium; the mass of the sun is so large that it contributes to 99.68 % of the total mass of the solar system .it gives us solar radiation [4].

The energy produced in the interior of the solar sphere, where temperatures reach many millions of degrees, must be transferred to the surface and then be radiated into space. A succession of radiative and convective processes occurs with successive emission, absorption, and re-radiation; the radiation in the sun’s core is in the X-ray and gamma-ray regions of the spectrum, with the wavelengths of the radiation increasing as the temperature drops at larger radial distances [4].

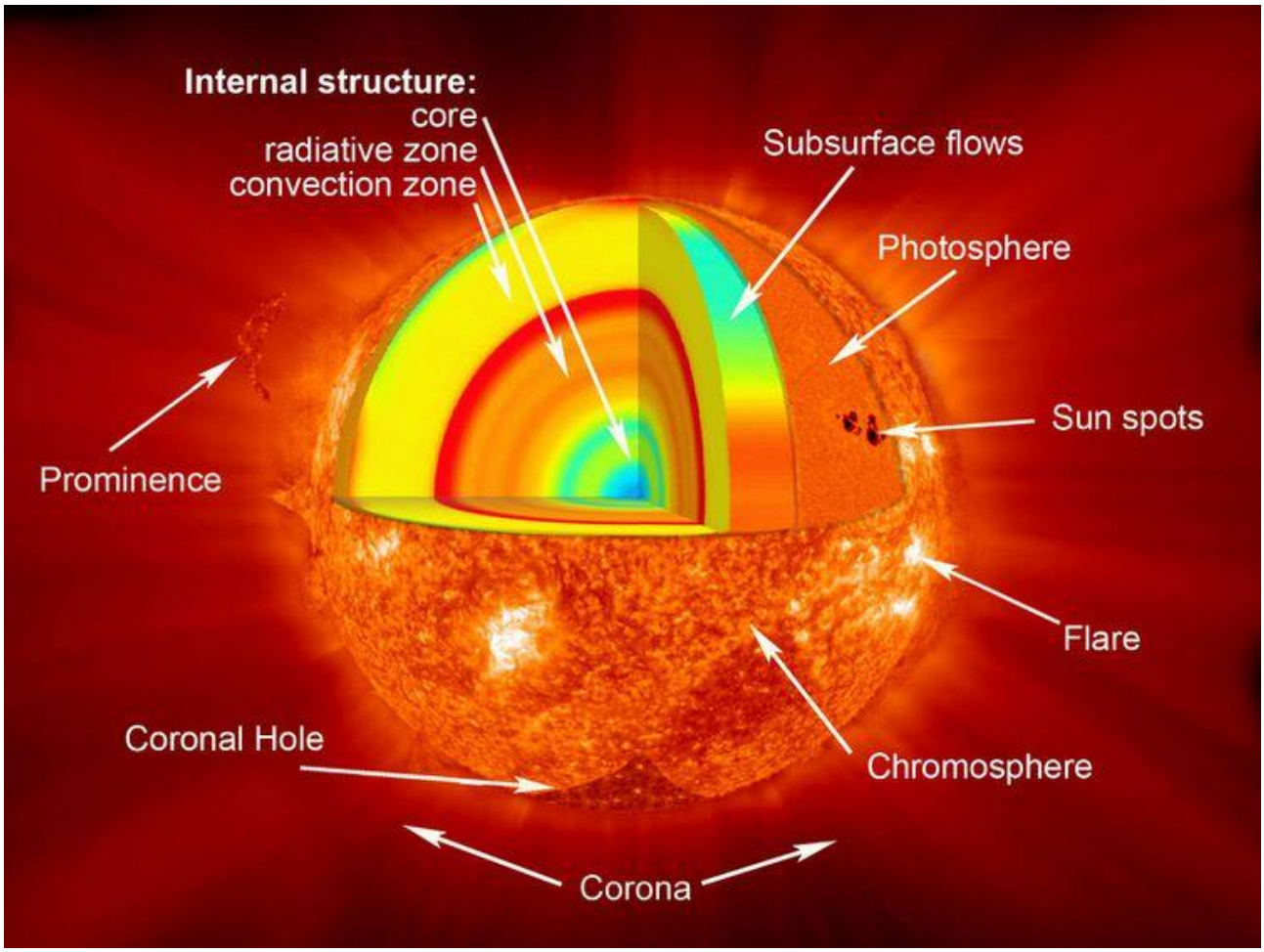

Figure (1-1) :The Sun

1.2.2 Sun-Earth geometry

Figure (1- 2) schematically shows the Sun -Earth geometry .the eccentricity of the Earth's orbit is such that the distance between the sun and earth varies by ±1.7% .at a distance of one astronomical unit ,1.495 $\times 10^{11}$m the average Sun – Earth distance, the sun is subtended by an angle of 32º .the radiation emitted by the sun and its spatial relationship to the Earth result in an almost fixed intensity of solar radiation outside the earth's atmosphere [5].

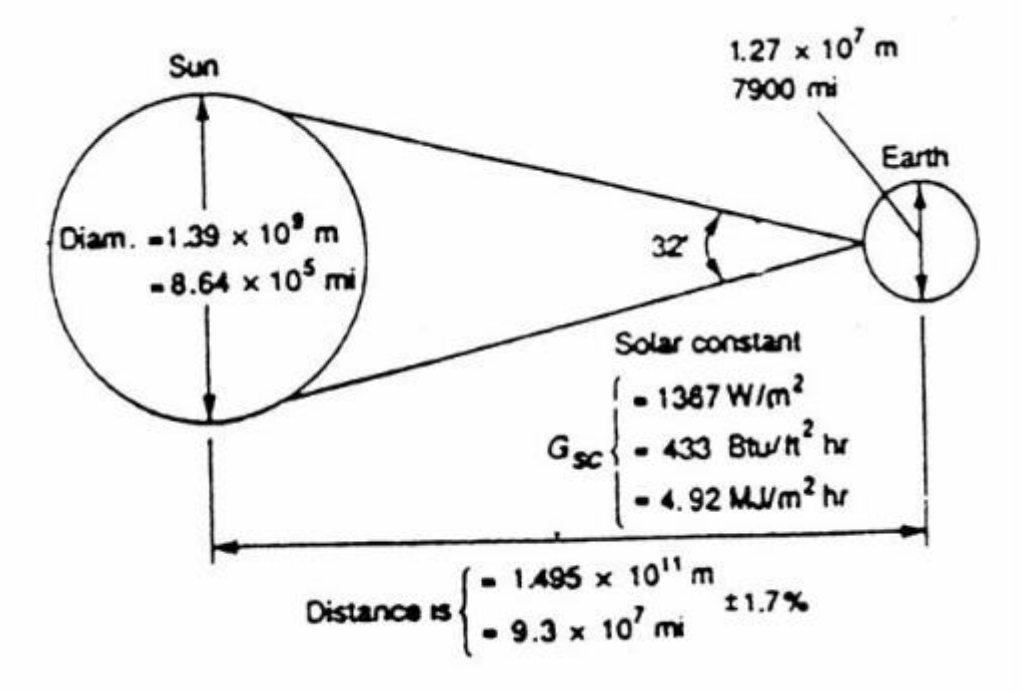

Figure (1- 2): Sun – Earth Relation.

1.2.3 Solar radiation

1.2.3.1. Definition of solar radiation

Solar radiation is emitted by the Sun as electromagnetic waves traveling at the speed of light (c). Each photon has a wavelength (λ) and its energy (E) is inversely proportional to the wavelength, according to Planck's theory, as shown in the following equation:

$$E = h.\upsilon = h.\frac{c}{\lambda} \qquad (1\text{-}1)$$

Where:

$\upsilon = \frac{c}{\lambda}$: is the wave frequency [Hz].

λ: is the wavelength

c: is the speed of light in vacuum, where: $c = 3 \times 10^8$ [m/s]

h: is the plank constant, where: $h = 6.62 \times 10^{-34}$[J.s]

1.2.3.2. Solar radiation spectrum

Solar radiation consists of a large electromagnetic spectrum, whose spectrum ranges from the short wavelengths (gamma rays) to long radio waves (Figure (1-3)). The parts of this spectrum that play a role in the interaction of solar radiation with the Earth's environment are essentially the infrared, visible, and ultraviolet bands, as well as the radiofrequency and microwave ranges [5]. That should be noted that 98% of solar radiation is emitted in wavelengths between 0.24 µm and 4 µm figure(1-4).

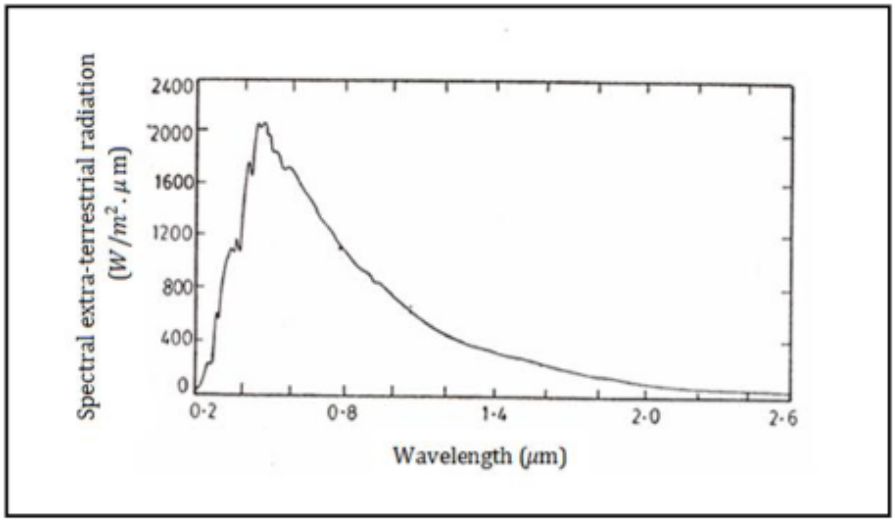

Figure (1 -3): Spectral distribution of solar radiation outside the atmosphere .

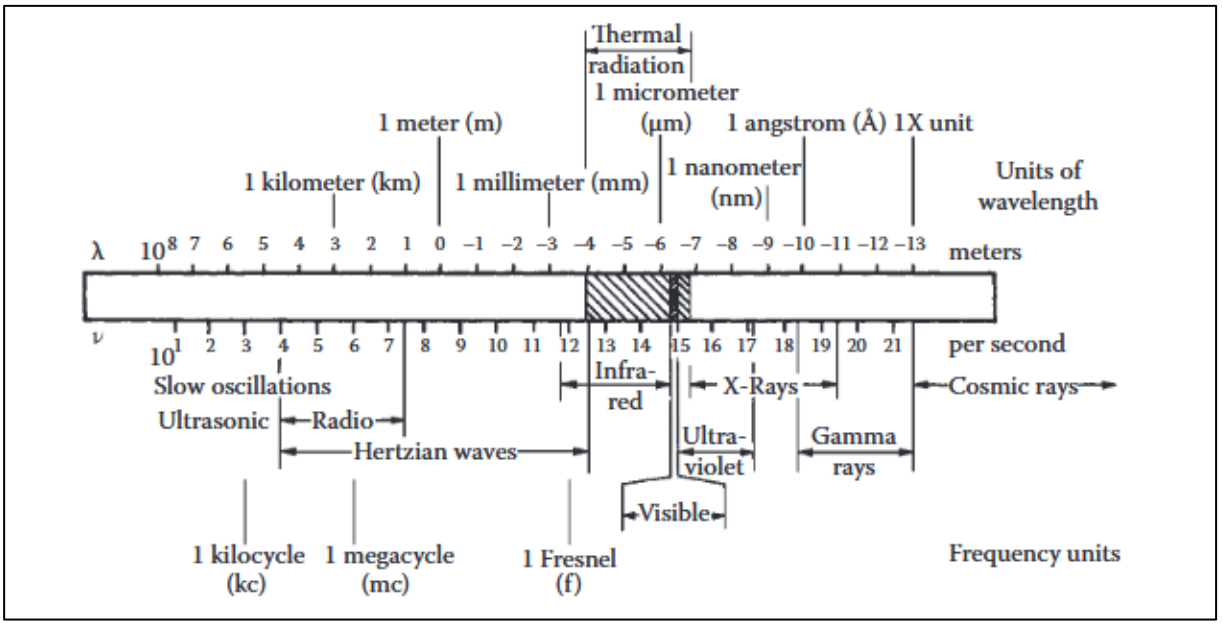

Figure (1-4): Electromagnetic radiation spectrum.

The different forms of solar radiation are represented in the table below. Solar radiation resembles blackbody radiation at temperature of 5777K within the spectral range λ = [0.25- 4] µm as it reaches the Earth's surface after partial absorption by various gases and water vapor in the atmosphere [5], as shown in figure (1-5).

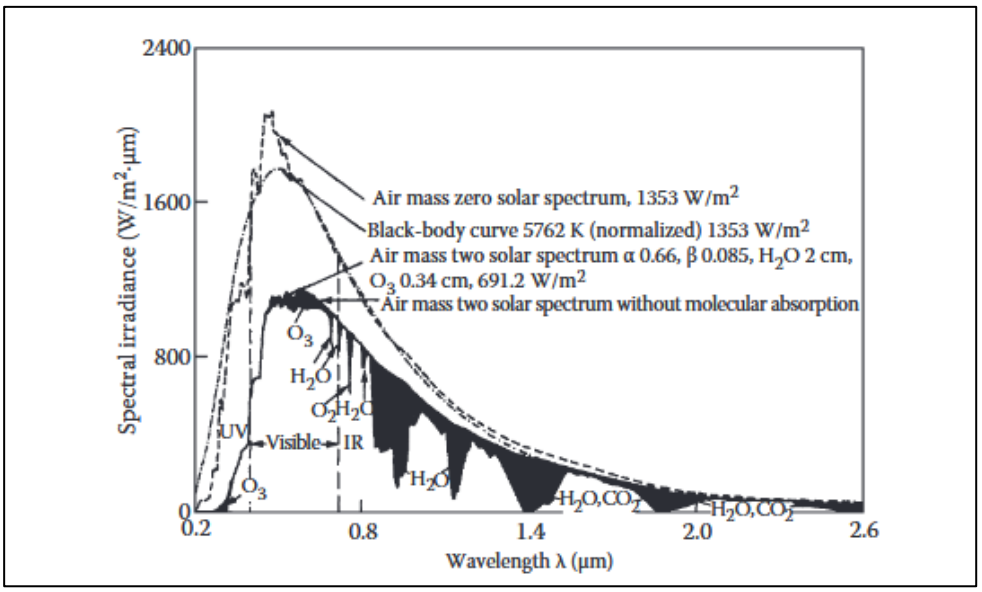

Figure (1-5): Extra-terrestrial solar radiation spectral distribution also shown are equivalent blackbody and atmosphere – attenuated spectra.

1.2.4 Factors affecting the distribution of solar radiation

Several factors affect the intensity of solar radiation and its variation during the day from sunrise to sunset, as well as its changes throughout the different seasons of the year.

1.2.4.1. Angle of incidence

The angle of incidence affects the intensity of solar radiation reaching the Earth's surface. This is because solar radiation with a regular incidence on the earth's surface is of high intensity, and its distribution is denser on the Earth's surface, on the one hand, and because the distance it travels is shorter compared to the rays with an oblique incidence, on the other hand. Therefore, it is less susceptible to losses due to the effects of refraction, scattering, and absorption that occur in the outer atmosphere.

1.2.4.2. Difference in the duration of sunshine by region

The duration of sunshine plays a major role in determining the amount of solar radiation received. Due to the tilt of the Earth's axis, the duration of sunshine in the Northern Hemisphere increases during summer and decreases during winter, while the opposite occurs in the Southern Hemisphere.

1.2.4.3. Atmospheric transparency

The presence of clouds, water vapor, dust, suspended solids, and ash in the atmosphere increases the absorption and scattering of solar radiation. Therefore, areas with high levels of dust and cloud cover receive less solar radiation than areas with clear air.

1.2.4.4. Topography of the region

Topography plays a major role, as the amount of solar radiation received varies from one region to another. The orientation and slopes of mountains influence the amount of solar radiation in temperate

and cold regions, where the Sun's rays reach the surface at an oblique angle. However, in tropical regions, this factor is less significant, as the Sun's rays reach the surface at a normal or nearly normal incidence throughout the year.

1.2.4.5. Albedo

Albedo is the percentage of direct solar radiation reflected from the Earth's surface back into space. The albedo percentage varies from one place to another depending on the latitude of the region and the nature of the surface, such as its composition (rocks, sand, limestone, etc.), color, the presence or absence of vegetation, the extent of snow cover, and its duration [7].

1.2.4.6. Solar constant

The solar constant expresses the amount of solar energy that a surface area of 1 m² located at a distant 1 astronomical unit distant (mean distance between the earth and the sun) exposed perpendicularly to solar radiation would receive if the earth's atmosphere did not exist .It is equal to ; G_{on} =1367 w/m² with an error of ±1% ,a value adopted by the world radiation center (WRC) .We can calculate the value G_{scn} as a function of the day number of year n by [5] :

$$G_{scn} = G_{on}\ [1 + 0.333 \cos(\frac{360n}{365})] \qquad (1\text{-}2)$$

Where is the extra-terrestrial radiation incident on the plan normal to the radiation on the nth day of the year. And give its variation during the year by the figure:

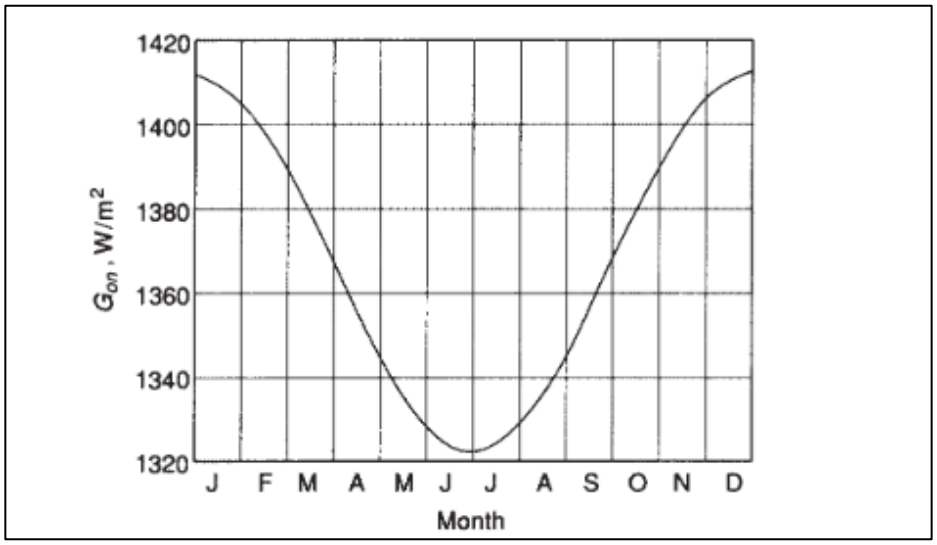

Figure (1-6): Variation of extra-terrestrial solar radiation with time of year.

1.2.5 Solar radiation at the earth's surface

We will then focus on the solar radiation intercepted by the Earth with the aim of calculating the flux received by a plane placed on a site on the earth's surface and oriented toward the sun.

Understanding this flux requires identifying the site on the earth's surface knowing the position and trajectory of the sun in the celestial vault, and knowing the earth's movements around the sun.

1.2.5.1. Earth's movements

The earth's path around the sun is an ellipse with the sun as one of its foci. The plane of this ellipse is called the ecliptic.

The eccentricity of this ellipse is small, meaning that the Earth and the sun vary by only ±1.7% compared to the average distance which is 149,675,106 km.

The Earth also rotates around itself along an axis (north pole, south pole). The alternation of days and nights is an immediate manifestation of this movement.

The plane perpendicular to the polar axis and passing through the center of Earth is called the equator. The polar axis is not perpendicular to the ecliptic: the equator and the ecliptic form an angle between them called the inclination, which is equal to: -23.45° and +23.45°. This inclination, combined with the Earth's rotational motion, ensures that the north poles are successively basked in the light, which causes the cycle of the seasons. [4]

The movements of the Earth around its axis and around the sun are shown schematically in figure (1-7).

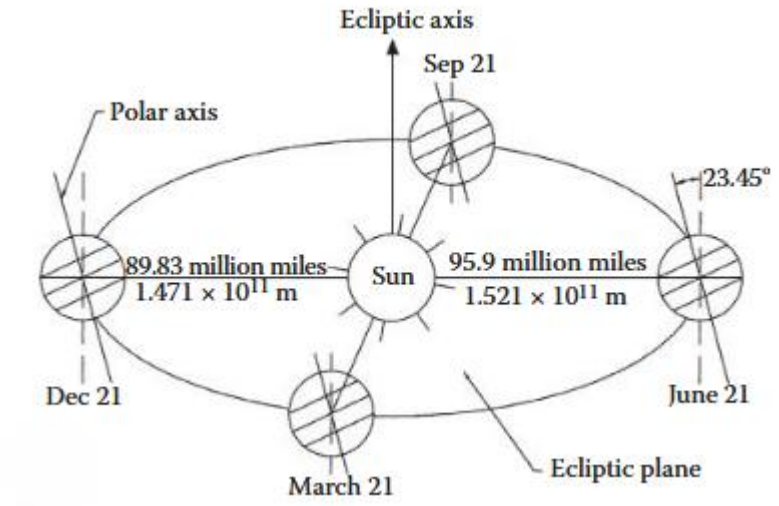

Figure (1-7): diagram of the movements of the earth around its axis and around the sun.

1.2.5.2. Locating a site on the earth's surface

It is possible to determine the position of a site on the Earth's surface using its geographic coordinates [5].

Geographic coordinates

To locate a location M on Earth, we need angular coordinates, which are the longitude and latitude figure (1-8).

Longitude

The longitude of a location λ corresponds to the angle made by the meridian plane passing through this location with a meridian plane chosen as the origin.

The meridian (the origin 0º) was chosen to be the plane passing through the Greenwich observatory. By convention, meridians located east given a (+) sign, and meridians located west of this meridian are given a (-) sign [11].

Latitude

the latitude of location φ corresponds to the angle with the equatorial plane made by the ray joining the centre of the Earth to this location. The Earth`s equator is therefore characterized by a latitude equal to 0º the north pole by latitude

+90º, and the south pole by latitude -90º. This sign convention assigns the (+) sign to all location in the Northern Hemisphere and the (-) sign to all location in the Southern Hemisphere fig (1-8) [5].

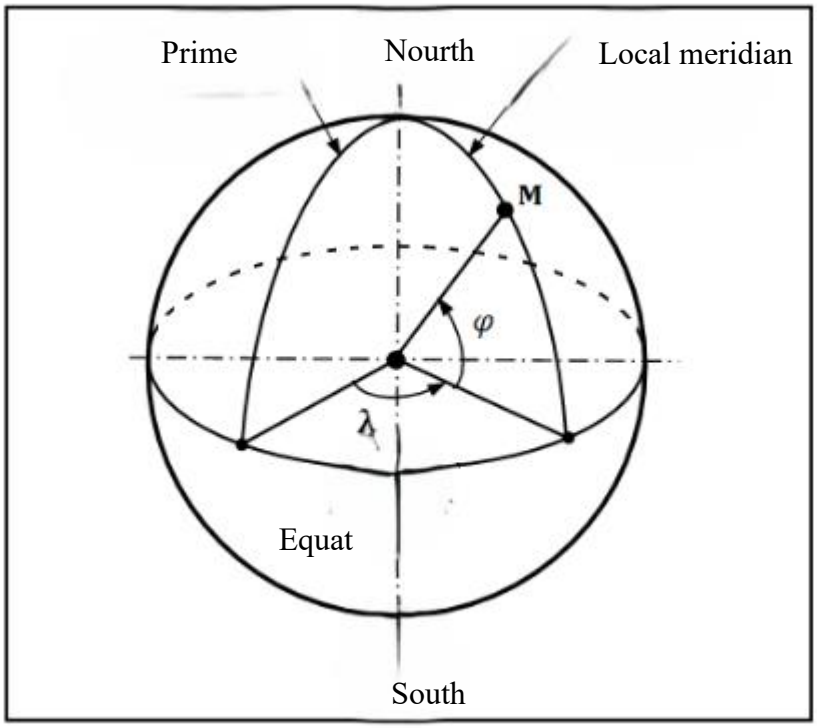

Figure (1-8) : Geographic coordinats.

1.2.6 Apparent motion of the sun

The position of the Sun at any time of the day and year is determined using two coordinate systems [5]: the equatorial coordinate system and the horizontal coordinate system.

1.2.6.1. Equatorial coordinate

The Sun’s motion is described relative to the Earth’s equatorial plane using two angles: the solar declination and the hour angle.

Solar declination

Solar declination δ is the angle formed between the direction of the Sun and its projection onto the equatorial plane. It varies throughout the year between −23.45° and +23.45°. It is zero at the equinoxes (March 21 and September 21), reaches a maximum at the summer solstice (June 21), and a minimum at the winter solstice (December 21) (Fig. (1-7). The value of the declination can be calculated using the following relationship [5]:

$$\delta = 23.45^{o}\sin\left[\frac{360}{365}(n + 284)\right] \qquad (1\text{-}3)$$

Where n is the number is the day of the year, counted from January 1st.

Hour angle (ω)

The hour angle of the sun is the angle formed by the meridian plane of location M and the angle that passes through the direction of the sun if we take the Greenwich meridian as the origin. It measures the sun's path across the sky and ranges between 0º and 360º. Its value is zero at solar noon, negative in the morning, positive in the afternoon, and increases by 15º per hour. The hour angle of the sun varies at every moment of the day according to the relationship [5]:

$$\omega = 15^{o}\,(TST - 12) \qquad (1\text{-}4)$$

Where

TST: is true solar time.

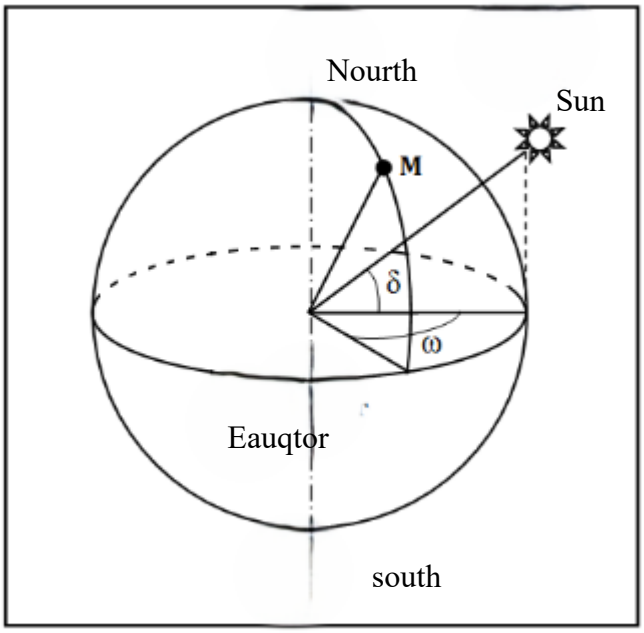

Figure (1-9): Equatorial coordinate.

The apparent motion of the sun as seen by an observer at a point of latitude φ north of the equator is shown in figure (1-10).

At solar noon, the angle between the direction of the sun and the vertical of the location is equal to (φ – δ).

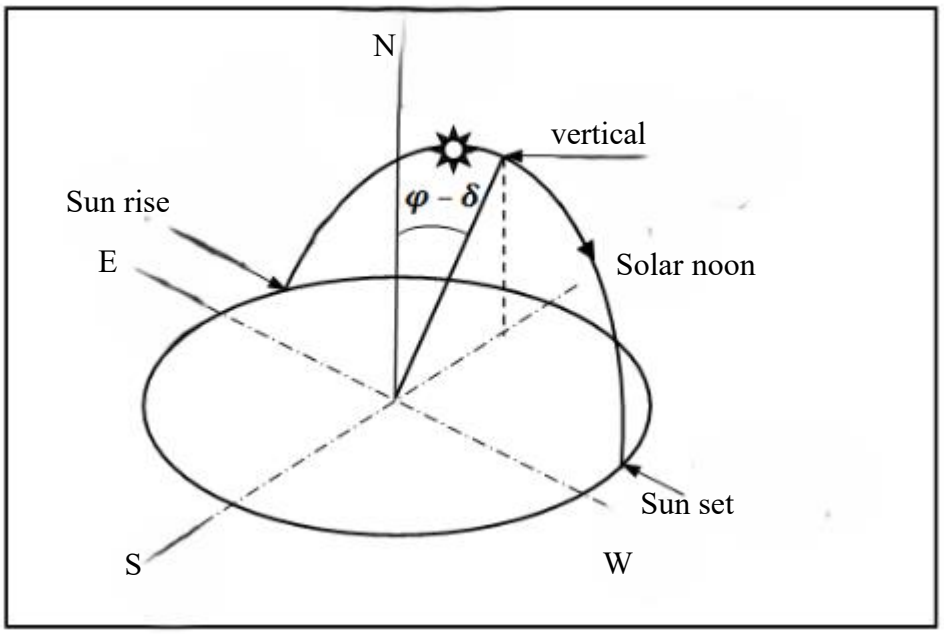

Figure (1-10): apparent motion of the sun observed from a point of latitude φ.

1.2.6.2. Horizontal coordinates

The Sun's motion is described relative to the horizontal plane at latitude φ by two angles (Fig. 10): The Sun's height h_s and the azimuth a_s.

Sun's height (h_s)

This is the angle between the direction of the Sun and its projection onto the horizontal plane.

The Sun's height varies at every moment of the day and throughout the year according to the following relation:

$$\sin(h_s) = \cos(\varphi)\cos(\delta)\cos(\omega) + \sin(\varphi)\sin(\delta) \qquad (1\text{-}5)$$

specifically:

$h_s = 0°$ at sunrise and sunset

$h_s = 90°$ at true solar noon

Azimuth (a_s)

This is the angle between the projection of the Sun's direction onto the horizontal plane and the south direction, measured positively toward the west [11].

The azimuth is related to the hour angle, altitude, and declination by the following expression:

$$\sin(a_s) = \frac{\cos(\delta)\sin(\omega)}{\cos(h_s)} \quad (1\text{-}6)$$

If the azimuth is to be expressed independently of the height h_s, the following relation can be used:

$$\tan(a_s) = \frac{\sin(\omega)}{\sin(\varphi)\cos(\omega) - \cos(\varphi)\tan(\delta)} \quad (1\text{-}7)$$

The azimuth angle varies between $-180°$and $+180°$, where:

- $a_s > 0$ toward the west
- $a_s < 0$ toward the east
- $a_s = 0$ toward the south

Knowledge of the azimuth angle is essential for calculating the angle of incidence of solar rays on a non-horizontal surface.

1.2.7 Solar time

Relations describing the motion of the Sun are expressed using solar time TS, which generally differs from the legal timeTL (watch time) at the location in question.

1.2.7.1. True solar time (TST)

True solar time, at a given instant and location, is the hour angle of the Sun. It is given by the following expression:

$$\text{TST} = 12 + \frac{\omega}{15} \quad (1\text{-}8)$$

- If ω = 0, TST= 12:00 pm.
- If ω < 0, the morning.
- If ω > 0, the afternoon.

1.2.7.2. Mean solar time (M.S.T)

The mean solar time is given by the following relation:

$$TST - TSM = E_t \quad (1\text{-}9)$$

Where E_t is the equation of time; it corrects the apparent solar time (TST) relative to the mean solar time (TSM).

The equations related to the movement of the sun use solar time TS, which generally differs from the legal time TL (watch time) of the location considered [7].

This difference is mainly due to:

The difference between the legal time TL and the civil time TCF of the time zone in which it is located

$$\text{C} = \text{TL} - \text{TCF} \quad (1\text{-}10)$$

The civil time TCF of the time zone is equal to universal time UT (solar time at the Greenwich meridian) plus the value of the time zone offset.

The variation in the earth's speed along its path around the sun introduces a corrective term called the equation of time, denoted Et [11].

$$E_t = 229.2\begin{bmatrix}0.000075 + 0.001868\cos(B) - 0.032077\sin(B)\\ -0.014615\cos(2B) - 0.04089\sin(2B)\end{bmatrix} \quad (1\text{-}11)$$

Where:

E_t:Equation of time (in minutes);

$$B = (n-1) \times \frac{360}{365}$$

n: Day number of the year.

1.2.7.3. Sunrise and sunset times

The duration of sunshine during a day depends on two important moments, sunrise and sunset. their equations are given as following:

Solar time of sunrise

$$TST_{sunrise} = 12 - \frac{\omega s}{15} \quad (1\text{-}12)$$

Solar time of sunset

$$TST_{sunset} = 12 + \frac{\omega s}{15} \quad (1\text{-}13)$$

The solar angle of sunrise is given by ωs and sunset, since the sun's elevation angle is zero in the equation Since h=0 which becomes sin(h)= 0 [7].

$$cos\omega s = -tan\delta.tan\varphi \Rightarrow \omega s = -arc\,cos(-tan\delta.tan\varphi) \quad (1\text{-}14)$$

1.2.8. Types of solar radiation

The atmosphere does not transmit all of the solar radiation it receives to the Earth's surface. Solar radiation reaching the ground encounters absorption and scattering phenomena as it passes through it, which contribute to its attenuation. At ground level, the total isolation received by a flat surface of any inclination is made up of three main components [7, 11]:

1.2.8.1. Direct radiation

Direct radiation is radiation that passes through the atmosphere unchanged. Its proportion is high on sunny days, while on cloudy days it is almost non-existent. The expression for the intensity of direct solar radiation coming from the sun to the Earth's surface perpendicularly after passing through the atmosphere is given by the following relation [7,11]:

$$I_b = I\,[a_0 + a_1\,e^{-K.AM}] \quad (1\text{-}15)$$

Where:

a_0, a_1 and k are empirical constants given by Duffie and Backman using that following relations:

$$a_0 = 0.94\ [\ 0.4237 - 0.00821\ (6 - Z)^{\,2}] \qquad (1\text{-}16)$$

$$a_1 = 0.98\ [\ 0.5055 - 0.00595\ (6.5 - Z)^{\,2}] \qquad (1\text{-}17)$$

$$K = 1.02\ [\ 0.2711 - 0.01858\ (2.5 - Z)^{\,2}] \qquad (1\text{-}18)$$

Where:

Z: altitude of the location above sea level, expressed in km.

AM: optical air mass.

I: solar constant.

In the case of direct solar radiation incident at an angle i on an inclined surface, it is given by the following relation

$$I_{bt} = I_b \cos i \qquad (1\text{-}19)$$

1.2.8.2. Diffuse radiation and reflected radiation

Diffuse radiation is the portion of solar radiation scattered by solid or liquid particles suspended in the atmosphere. It has no preferred direction. The amount of this radiation is 10 % when the sky is clear, and 100% when the sky is overcast [5].

The expression for the intensity of diffuse solar radiation is given by the following relation [7]:

$$I_{(d)} = I.sin\ h\ [\ 0.2710 - 0.2939\ (\ a_0 + a_1 exp(-K.AM\ ))] \qquad (1\text{-}20)$$

In other hand, the reflected radiation is the portion of solar radiation reflected by the Earth's surface in a diffuse manner. The intensity of reflected solar radiation is given by the following relation [5,7]:

$$I_r = \rho\ I_g \sin\ (h) \qquad (1\text{-}21)$$

Global radiation is equal to the superposition of the three components: direct, diffuse, and reflected [5].

1.3. Solar tracking

In order to maximize the amount of direct solar radiation in various optical and thermal applications, the aperture of the solar collector must follow the path of the Sun so that the Sun's rays remain perpendicular or nearly perpendicular to the aperture throughout the duration of the sun`s exposure. There are several types of solar tracking [7]

1.3.1. Tracking with two rotation axes

In this case, the solar collector is moved horizontally to track the sun's azimuth and moved vertically to follow the Sun's elevation, so that the Sun's rays always remain perpendicular to the aperture

surface. This type of tracking is suitable for parabolic dish systems, as it represents the ideal case in terms of maximizing solar energy capture on one hand, and is practically achievable due to the low rotational inertia of the dish on the other hand. In this case, the angle of incidence is zero: θ = 0 [7].

1.3.2. Single axis tracking

Tracking with a single axis of rotation comes in two types: either elevation tracking or azimuth tracking.

1.3.3. Solar elevation tracking

In this case, the solar collector is moved vertically to follow the Sun's elevation, so that the Sun's rays always fall perpendicularly onto the aperture surface. The azimuth angle is fixed at α = 0, meaning the collector is oriented toward the south (in the northern hemisphere), which is considered the optimal position. The elevation angle of the collector equals the solar elevation angle [7].

1.3.4. Solar Azimuth tracking

In this case, the solar collector is moved horizontally to follow the Sun's azimuth. It is oriented eastward at sunrise and gradually moves westward throughout the day. The azimuth angle of the collector matches the Sun's azimuth angle, while the elevation angle of the collector is fixed at an average value [8]:

$$\beta = \varphi - \delta \qquad (1\text{-}22)$$

This is the difference between the latitude angle (Φ) and the solar declination angle (φ), considered the most suitable fixed angle during the day.

1.3.5. Non-tracking case (fixed solar collector)

In this case, the angle of incidence i between the solar beam and the normal to the surface of solar collector's aperture depends on several angles:

- ❖ The latitude of the location.
- ❖ The solar declination angle.
- ❖ The azimuth angle.
- ❖ The tilt.
- ❖ The angle of the collector surface from the horizontal (β).

This relation is given by the John and al. equation [11]

$$\text{Cos i} = \sin\varphi\,(\sin\delta \cdot \cos\beta + \cos\delta \cdot \cos a \cdot \cos\omega \cdot \sin\beta) + \cos\varphi\,(\cos\delta \cdot \cos\omega \cdot \cos\beta - \sin\delta \cdot \sin a \cdot \sin\beta) + (\cos\delta \cdot \sin a \cdot \sin\omega \cdot \sin\beta) \qquad (1\text{-}23)$$

When the aperture surface is horizontal (β = 0), the angle of incidence become:

$$\cos i = \cos\varphi \cos\delta \cos\omega + \sin\varphi \sin\delta \qquad (1\text{-}24)$$

For a collector oriented toward the south (azimuth angle a = 0) and tilted from the horizontal by an angle β the angle of incidence becomes:

$$cos\, i = cos\,(\varphi - \beta)\,.cos\,\delta\,.cos\,\omega + sin\,(\varphi - \beta)\,.sin\,\delta \qquad (1\text{-}25)$$

and for a collector tilted by an angle equal to the latitude (β = φ) the relation becomes:

$$cos\, i = cos\delta\,.cos\,\omega \qquad (1\text{-}26)$$

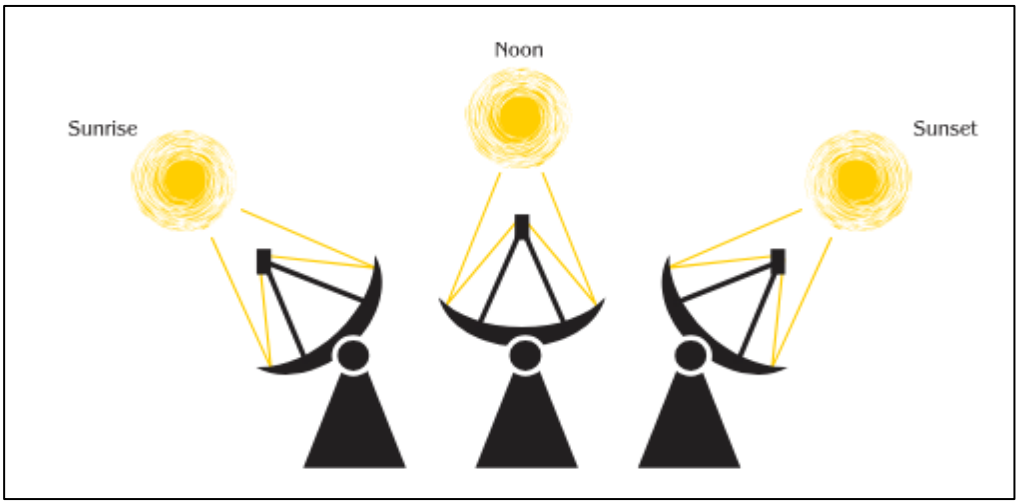

Figure (1-11): The tracking.

Due to the weak intensity of solar radiation in industrial applications, there is an urgent need to increase the radiation intensity. This is achieved through solar concentrators that receive direct radiation and collect it towards the focus, thanks to the geometric design of the reflector. Thus, we obtain at the focus that we will learn about in the following paragraphs.

1.4. Solar concentrator

Solar concentrators are among the most efficient systems for harnessing solar energy. Their core principle relies on collecting direct solar radiation and directing it toward a specific focal point-either point or linear-thereby significantly increasing the thermal radiation intensity.

The high-intensity radiation is utilized in a wide range of industrial applications, whether for converting solar energy into thermal energy or for use in photonic (optical) conversion processes. The efficiency of these systems is largely attributed to the engineering design of the reflector, which enables precise concentration of sunlight due to its carefully calculated curvature [12].

The operating principle of solar concentrators involves receiving direct solar radiation through an aperture. The incident rays strike the reflector's surface and are redirected to converge at the focal point. The intensity of the concentrated solar radiation can increase by tens to thousands of times

compared to the original, and this increase is quantified by the concentration ratio, which is defined as the ratio of the aperture area A_{ap} to the receiver area A_r [8]:

$$C = \frac{A_{ap}}{A_r} \quad (1\text{-}27)$$

1.4.1. Parabolic trough

The most widely used type of concentrator in concentrated solar power (CSP) systems accounting for approximately 96% of all installed CSP capacity. This technology employs a linear parabolic reflector to focus sunlight onto an absorber tube positioned along the focal line of the mirror. Inside this tube, a heat-transfer fluid is circulated and heated to temperatures ranging from 150˚C to 350˚C [4, 8].

Figure (1-12): Parabolic trough [4].

Figure (1-12): parabolic trough.

1.4.2. Solar power towers

Solar power tower utilizes a field of dual-axis tracking mirrors, known as heliostats, which are strategically positioned around a central tower. These heliostats reflect and concentrate sunlight onto a receiver located the top of the tower. The receiver contains a working fluid that is heated by the concentrated solar energy to extremely high temperatures, typically ranging from 500˚C to as high as 1000˚C [4, 8].

Figure (1-13): solar power towers.

1.4.3. Fresnel concentrator

Another type of solar concentrator, which utilizes an array of flat mirrors to focus sunlight. Compared to traditional parabolic mirrors, flat mirrors offer a more compact arrangement, enabling greater reflective surface area within the same spatial footprint. This design not only enhances the overall sunlight capture but also significantly reduces material and manufacturing costs, making Fresnel concentrators a more economical and efficient alternative [4, 8].

Figure (1-14): Fresnel concentrator.

1.4.4. Dish-Stirling system

A Dish Stirling system, also known as a Dish Engine system, utilizes a parabolic reflector to concentrate solar radiation onto a focal point, where a working fluid absorbs the thermal energy and is heated to temperatures of approximately 500˚C, the dish-Stirling system currently holds the record for the highest efficiency among solar thermal power technologies [4, 8].

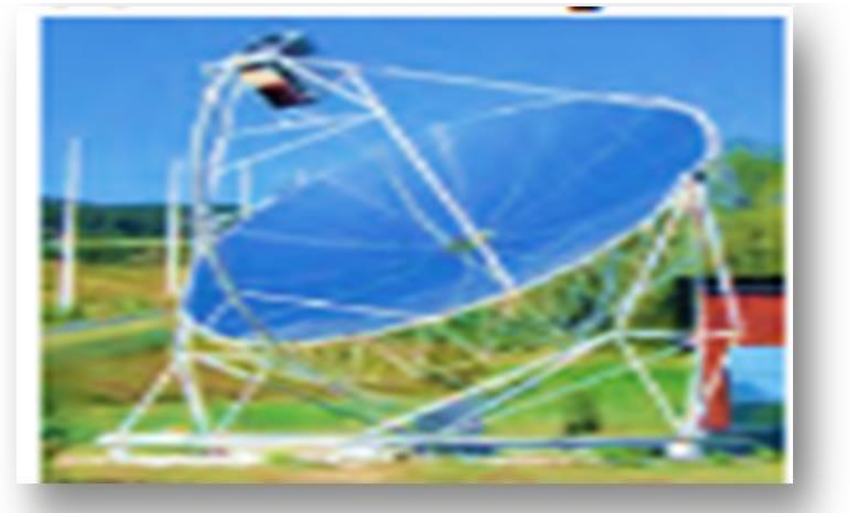

Figure (1- 15): The dish-Stirling system.

1.4.4.1. Components

a. Reflector

The surface of the reflector is shaped as a paraboloid and coated with a reflective material such as silver or aluminum in order to reflect and concentrate solar radiation at the focal point [7,12].

b. Receiver

The receiver is placed at the focal point to absorb the concentrated solar radiation. Thermal energy conversion takes place at this location, such as in the case of a Stirling engine used as a thermal receiver, or photovoltaic conversion as in the case of laser materials used as photovoltaic receivers [7,12].

1.4.4.2. Geometry of the parabolic shape

a. Area of a dish

A parabolic reflector is formed by rotating a parabola around its axis. The equation of a paraboloid of revolution, obtained by rotating a parabola about its axis of symmetry (the Z-axis) is given by [12]:

$$X^2 + Y^2 = 4.f.Z \qquad (1\text{-}28)$$

$$Z = \frac{a^2}{4.f} \qquad (1\text{-}29)$$

The surface area of paraboloid is calculated by integrating the equation:

$$dA_s = 2.\pi.a\sqrt{dz^2 + da}\ (1\text{-}28) \qquad (1\text{-}30)$$

$$\mathrm{d}A_s = 2.\pi.\mathrm{a}\sqrt{\left(\frac{a}{2f}\right)^2 + 1.da} \qquad (1\text{-}31)$$

the surface area of paraboloid is given by:

$$A_s = \int_0^{\frac{d}{2}} dA_s = \frac{8}{3}.\pi.f^2[[\left(\frac{d}{4f}\right)^2 + 1]^{3/2} - 1] \quad (1\text{-}32)$$

While the area of the hole represents the area of a disk with radius d:

$$A_a = \frac{\pi.\mathrm{d}^2}{4} \quad (1\text{-}33)$$

b. Edge angle

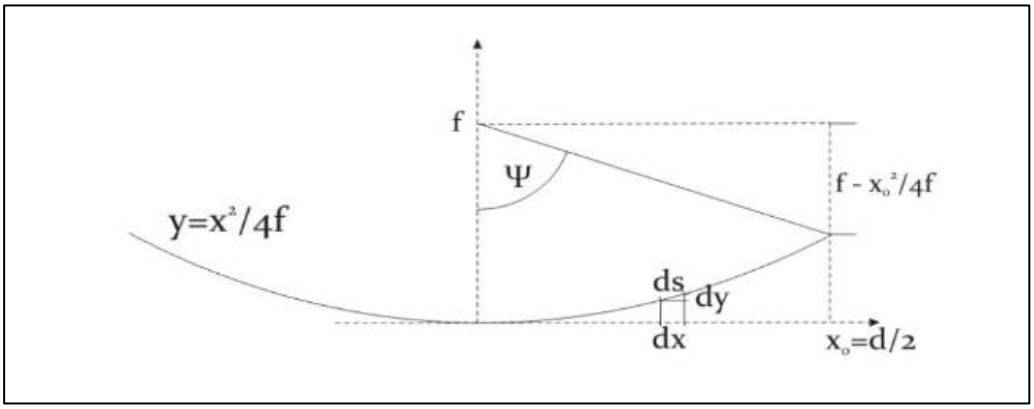

figure (1-16): Diagram of the edg angle.

$$tan\psi = \frac{X_0}{f - \frac{X_0^2}{4f}} \quad (1\text{-}34)$$

$$tan\psi = \frac{\frac{d}{f}}{2 - \frac{1}{8}(\frac{d}{f})^2} \quad (1\text{-}35)$$

1.4.4.3. Photometric study

The solar irradiation falling on the focus (the receiver) after the concentration process:

$$G_h = I \times \rho \times C \quad (1\text{-}36)$$

The spectral solar irradiation transmitted to the receiver through the filter in the range $(\lambda_1 \rightarrow \lambda_2)$ is given by the relation:

$$G_{(\lambda_1 \rightarrow \lambda_2)} = I_{(\lambda_1 \rightarrow \lambda_2)} \times \rho^0 \times \mathrm{C} \quad (1\text{-}37)$$

Where the spectral intensity of the direct solar radiation is given by the relation

$$I_{0(\lambda_1 \rightarrow \lambda_2)} = E_{(\lambda_1 \rightarrow \lambda_2)}[\,1 + 0.033.cos[(N_J)\frac{360}{365}]] \quad (1\text{-}38)$$

From planck's relation which gives the energy of radiation emitted by a black body:

$$E_{(\lambda_1 \to \lambda_2)} = \left(\frac{D_s}{D_{s,T}}\right)^2 \int_{\lambda_1}^{\lambda_2} \frac{C_1}{\lambda^5 [e^{(C_2/\lambda T} - 1]} d\lambda \qquad (1\text{-}39)$$

Where: $C_1 = 2\pi hc^2$ and $C_2 = \frac{hc}{K}$

D_s is the diameter of the sun.

$D_{s,T}$ is the diameter between the sun and the earth.

1.4.4.4. Optical efficiency of a parabolic dish

When the parabolic dish is fixed (non-tracking) and oriented towards the south (solar azimuth angle is zero), and its tilt angle β is set equal to the geographic latitude of the location φ, this configuration represents the optimal fixed orientation for year around solar collection.

.

In this setup, the angle of incidence of the solar beam relative to the normal to the dish surface is given by the following relation:

$$\cos i = \cos \delta \times \cos \omega \qquad (1\text{-}40)$$

The power received by the concentrated solar receiver, expressed in watts (W), is given by:

$$g = I \rho^0 \cos i \left(\frac{\pi d^2}{4}\right) \qquad (1\text{-}41)$$

In the case of a spectral filter, the power of the radiation concentrated on the solar receiver, expressed in watts (W), becomes:

$$g_{(\lambda_1 \to \lambda_2)} = I_{(\lambda_1 \to \lambda_2)} \rho^0 \cos i \left(\frac{\pi d^2}{4}\right) \qquad (1\text{-}42)$$

While the intensity of the solar beam received by the aperture, in units of (w):

$$g_0 = I . \left(\frac{\pi d^2}{4}\right) \qquad (1\text{-}43)$$

The optical efficiency of the parabolic dish is defined as the ratio between the solar radiation that reaches the receiver and the solar radiation that is reflected to the aperture and it is given in the presence of the spectral filter by the following relation:

$$\eta_{\text{opt}} = \frac{g_{(\lambda_1 \to \lambda_2)}}{g_0} = \rho^0 \cos i \frac{I_{(\lambda_1 \to \lambda_2)}}{I} \qquad (1\text{-}44)$$

By substituting the relation for the angle of incidence, we obtain:

$$\eta_{\text{op}} = \rho^0 \cos \delta \cos \omega \frac{I_{(\lambda_1 \to \lambda_2)}}{I} \qquad (1\text{-}45)$$

The intensity of the solar radiation reaching the receiver, in unit of w/m² is given by the relation:

$$G_{(\lambda_1 \to \lambda_2)} = \frac{g_{(\lambda_1 \to \lambda_2)}}{\left(\frac{\pi d_f^2}{4}\right)} = I_{(\lambda_1 \to \lambda_2)}\, \rho^0 \cos\, i \left(\frac{d}{d_f}\right)^2 \quad (1\text{-}46)$$

Therefore, we obtain:

$$G_{(\lambda_1 \to \lambda_2)} = I_{(\lambda_1 \to \lambda_2)}\, \rho^0 \cos\, \delta \cos\, \omega\, C \quad (1\text{-}47)$$

Where the geometric factor of the parabolic dish is given by:

$$C = \frac{A_{ap}}{A_r} = \left(\frac{d}{d_f}\right)^2 \quad (1\text{-}47)$$

Chapter 2:

Laser and solar laser

Chapter 2: Laser and solar laser

The history of the laser began in 1917, when Albert Einstein published his famous work on the absorption and emission of light. In this work, he introduced a new process known as stimulated emission, distinguishing it from spontaneous emission. LASER is an acronym for Light Amplification by Stimulated Emission of Radiation. These fundamental studies laid the theoretical foundation for the development of masers (Microwave Amplification by Stimulated Emission of Radiation) and later lasers [13, 16].

However, it was not until 1955 that the first maser was successfully built. In 1958, a study demonstrated the possibility of constructing an oscillator operating at optical and infrared frequencies by extending the principles of the Laser to the optical region of the electromagnetic spectrum [13].

2.1. Basic components of a laser

A laser is a highly specialized light source that operates by amplifying and directing electromagnetic radiation into an intense, narrow beam. This beam is characterized by its coherence, monochromaticity, and high directionality, allowing it to propagate over long distances in a straight line with minimal divergence.

The structure of a laser system is composed of three essential components, each playing a critical role in the generation and amplification of laser light [16]:

2.1.1 Active medium

The active medium in a laser, often referred to as the gain medium, can be a solid, liquid, or gas. This medium contains atoms or molecules characterized by a well-defined energy level diagram. Within this diagram, a metastable energy level exists, corresponding to an allowed transition between two energy states.

This transition occurs relatively slowly, allowing a large number of excited atoms to accumulate in the metastable state. As a result, a condition known as population inversion is achieved, which is a fundamental requirement for stimulated emission to occur.

2.1.2 Optical resonator

The optical resonator, also called a resonant cavity**,** is one of the core components of a laser system. In its simplest configuration, it consists of two parallel mirrors facing each other, with the active medium placed between them.

The resonator reflects the photons generated within the active medium, causing them to bounce back and forth millions of times per second. Each time the photons pass through the active medium, they stimulate excited atoms to emit additional photons through the process of stimulated emission. This repeated amplification ultimately leads to the formation of a coherent and highly focused laser beam.

2.1.3 Pumping source

Pumping is the process of transferring energy from an external source to the active medium within a laser system. This energy excites atoms or molecules in the medium, causing them to transition to higher levels.

As a result of this excitation, the population of the particles becomes unevenly distributed, with more atoms occupying excited states than lower ones a condition known as population inversion. Achieving this inversion is a critical requirement for the initiation of stimulated emission, which enables laser operation.

Several pumping methods can be employed depending on the laser design, including:

- **Optical pumping** (using light sources such as flash lamps or lasers)
- **Electrical pumping** (using electric current or discharge, commonly in gas lasers)
- **Chemical pumping** (using energy from exothermic chemical reactions)

Each method is selected based on the nature of the active medium and the desired laser performance characteristics.

2.2. Principle of laser operation

2.2.1. Radiation–Matter interaction

A comprehensive understanding of laser operation begins with an analysis of the interaction between electromagnetic radiation and matter, specifically focusing on the mechanisms of photon absorption and emission within the atoms or molecules of the active medium.

The fundamental principle of optical amplification and, consequently, laser generation arises from this interaction. When matter interacts with electromagnetic radiation, transitions occur between discrete atomic or molecular energy levels. These transitions may be:

- Radiative, involving the absorption or emission of photons.
- Non-radiative, where energy is transferred without photon exchange.

As photons travel through the active medium, they may be absorbed by ions or atoms, elevating them to excited energy states. Subsequently, these particles return to their lower or ground energy states, emitting the surplus energy as photons.

These processes are governed by two key phenomena photon absorption and photon emission which constitute the basis of all radiative interactions. Together, they form the theoretical foundation of laser physics, enabling the controlled generation of coherent, monochromatic, and highly directional light [7].

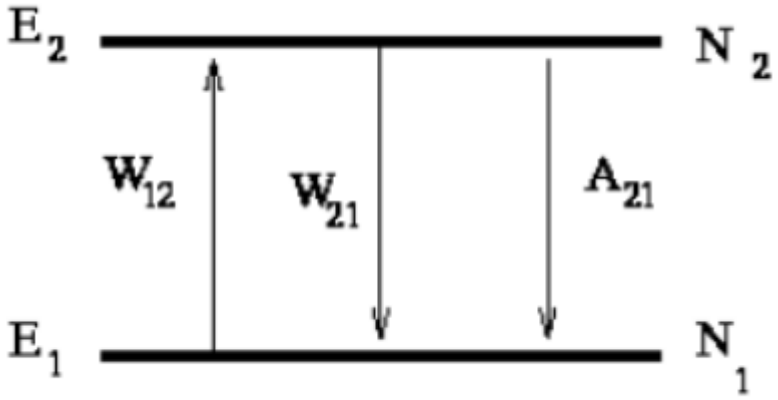

Figure (2-17): The main mechanisms of radiation intraction with mater.

2.2.2. Photon absorption

When particles (atoms, ions, molecules) are exposed to electromagnetic radiation, they can absorb photons whose energy corresponds to the difference between two quantized energy levels within the particle. This energy promotes electrons from lower energy states to higher energy states, a process known as electronic excitation. Photon absorption can occur only when the photon's energy exceeds the energy gap between the initial and final electronic states, expressed by the equation [13]:

$$\Delta E = E_2 - E_1 = h\nu \qquad (2\text{-}1)$$

where:

ΔE is the energy of the photon,

h is Planck's constant,

ν is the frequency of the radiation,

- E_1 and E_2 represent the lower and upper energy levels, respectively.

2.2.3. Diagram of the absorption process

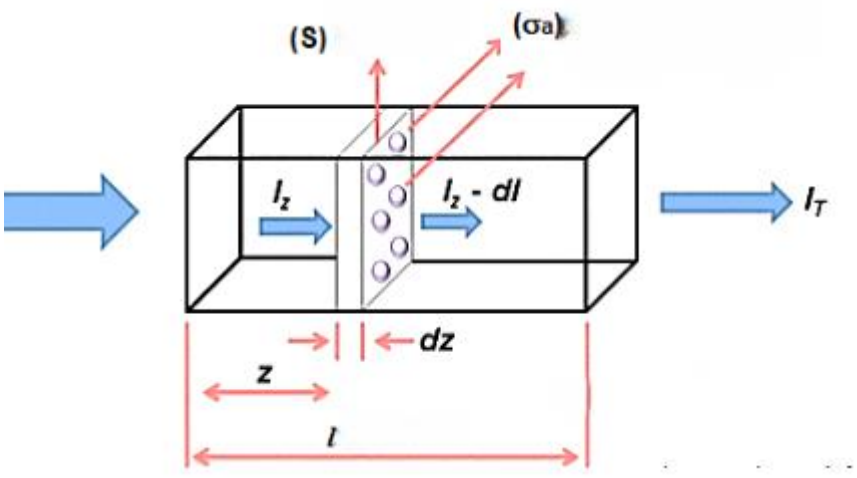

Figure (2- 18): Diagram of the absorption process.

The intensity of the beam decreases during propagation through the absorbing medium according to the following equation:

$$\frac{dI(Z)}{dZ} = -\sigma_a(Z)\, N_1 \qquad (2\text{-}2)$$

Assuming that the absorption probability is weak, the population in the excited state E_2 is negligible compared to the total population N (in cm^{-3}), therefore, $N \approx N_1$. The remaining intensity of the incident beam emerging from the absorbing medium of thickness l is given by the relation

$$I(l) = I_0 e^{-\sigma_a N l} = I_0 e^{-\alpha l} \qquad (2\text{-}3)$$

Where $\alpha = \sigma_a . N$ is the absorption coefficient, expressed in units of (cm^{-1}). It can be interpreted as the probability of absorption per unit length.

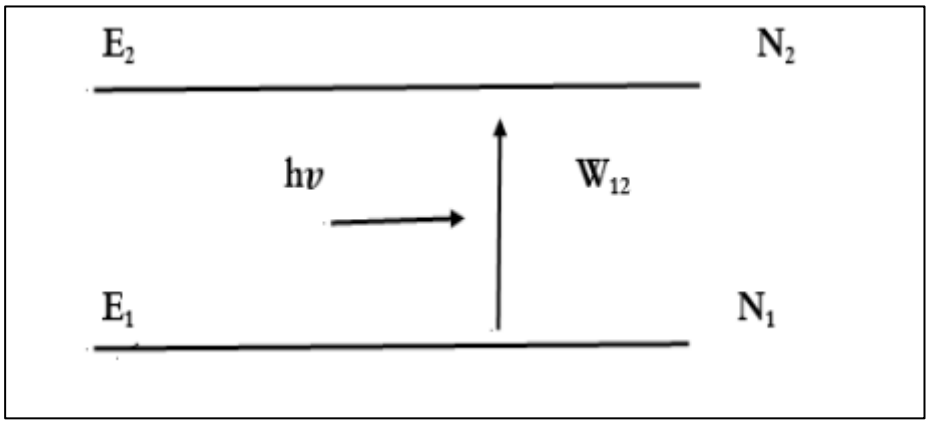

Figure (2-19): A diagram illustrating the absorption process.

The variation of the population in the energy level E_2 over time allows us to determine the excitation probability per unit time, denoted by w_{12}

$$\frac{dN_2(dt)}{dt} = \sigma_a D N_2(dt) = w_{12} N_2(\mathrm{dt}) \qquad (2\text{-}4)$$

Where D represents the photon flux per unit area, the number of photons passing through a cross-sectional area per second, and is given by the following relation:

$$\mathrm{D} = \frac{I}{h\upsilon} \qquad (2\text{-}5)$$

where I is the intensity of the incident radiation (power per unit area)

The transition probability from the state E_1 to the excited state E_2 can also be expressed using the Einstein coefficient B_{12} , as follows:

$$w_{12} = B_{12}\, \rho(\upsilon) \qquad (2\text{-}6)$$

Where ρ(ν) denotes the spectral energy density at frequency, representing the energy per unit volume per unit frequency. It is measured in (J.s.m^{-1}).

2.2.4. Spontaneous emission

Excited particles do not remain in their higher energy state indefinitely. Over time, they spontaneously decay to a lower energy level typically the ground state releasing the excess energy in the form of emitted electromagnetic radiation. This process is known as spontaneous emission, and it involves a transition from the excited state E_2 to the lower energy state E_1.

The average time a particle spends in the excited state before spontaneously decaying is called the excited-state lifetime, denoted by τ.

.

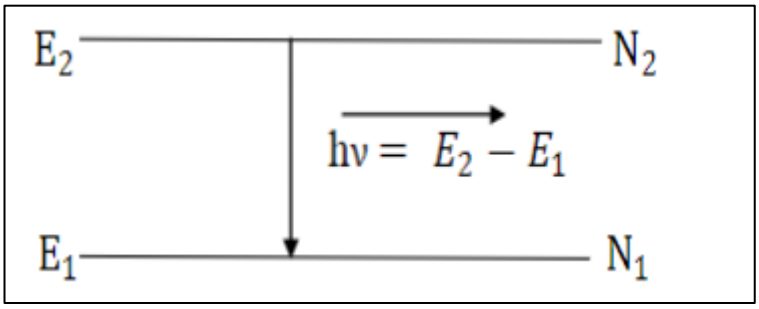

Figure (2-20): A diagram illustrating the spontaneous emission process.

The change in the population N_2 of the excited state can be expressed in terms of the Einstein coefficient A_{21} , which represents the probability of spontaneous emission per unit time, by the following equation

$$\frac{dN_2}{dt} = A_{21}N_2 \qquad (2\text{-}7)$$

We easily arrive at the following equation:

$$N_2 = N_0 e^{-A_{21}\,t} \qquad (2\text{-}8)$$

In the simple case of a two-level system, the radiative lifetime is defined as follows:

$$\tau_{rad} = \frac{1}{A_{21}} \qquad (2\text{-}9)$$

τ_{rad} : is the radiative lifetime (or excited-state life time)

There are excitation processes that do not involve photon emission, known as non-radiative processes, which contribute to the depopulation of the excited state without the generation of light. These are characterized by their own non-radiative lifetime.

In atomic or ionic systems with multiple energy levels such as an excited state E_m and several lower levels E_j multiple spontaneous transitions can occur from E_m to each E_j. Each of these transitions is associated with an Einstein coefficient A_{mj}, representing the probability per unit time for a spontaneous emission from E_m to E_j[7].

The total spontaneous emission probability from the excited state is given by the sum of all such coefficients:

$$\sum_j A_{mj}$$

Accordingly, the radiative lifetime is defined as:

$$\tau_{rad} = \frac{1}{\sum_j A_{mj}} \quad (2\text{-}10)$$

This lifetime represents the average time an atom or ion remains in the excited state before spontaneously emitting a photon and transitioning to a lower energy level.

2.2.5. Stimulated emission

Stimulated emission occurs when particles are induced to transition from a higher energy level to a lower one by an incident photon whose energy precisely matches the energy difference between the two levels. As a result of this transition, a second photon is emitted that is identical to the stimulating photon in terms of energy, phase, direction, and polarization. This coherent amplification of light is the fundamental principle behind laser operation [14,13].

For stimulated emission to dominate over absorption, a condition known as population inversion must be achieved. This requires that the number of particles in the excited state N_2 exceeds that in the lower energy state N_1 (N_2>N_1).

This phenomenon can be statistically modelled by incorporating the probability of stimulated emission, as described by the Einstein coefficients. Specifically, the rate of stimulated emission is proportional to the spectral energy density ρ(ν) and is governed by the Einstein coefficient B_{21}:

$$w_{21}(\upsilon) = B_{21}\ \rho(\upsilon) \quad (2\text{-}11)$$

The time-dependent change of the population N_2 in this case is

$$\frac{dN_2}{dt} = -\ B_{21}\ \rho(\upsilon)\ N_2 \quad (2\text{-}12)$$

The emission cross-section σ_e is defined as follows

$$\frac{dN_2}{dt} = -\ w_{21}N_2 = \frac{\sigma_e I_p}{h\upsilon}\ N_2 \quad (2\text{-}13)$$

Where: I_p is the intensity of the incident beam (w/cm²)

In the case of a two-level system, we have:

$$\frac{dN_2}{dt} = -\ w_{12}N_1\ -\ (\ w_{21}\ +\ A_{21})\ N_2 = -\ \frac{dN_1}{dt} \quad (2\text{-}14)$$

In the steady-state where ($\frac{N_i}{dt} = 0$), we find:

$$\frac{N_2}{N_1} = \frac{w_{12}}{w_{21}+A_{21}} \quad (2\text{-}15)$$

By substituting $w_{12} = B_{12}\rho(\nu)$and $w_{21} = B_{21}\rho(\nu)$into the above equation, we obtain

$$\frac{N_2}{N_1} = \frac{B_{12}\rho(\nu)}{B_{21}\rho(\nu) + A_{21}} \quad (2\text{-}16)$$

The energy density of the beam per unit area can be expressed as:

$$\rho(\upsilon) = \frac{A_{21}}{B_{21}} \cdot \frac{1}{(\frac{B_{12}}{B_{21}}\frac{N_1}{N_2} - 1)} \quad (2\text{-}17)$$

According to Planck's law:

$$\rho(\upsilon) = \frac{8\pi n^3 \upsilon^2}{c^3} \cdot \frac{h\upsilon}{e^{\frac{h\upsilon}{KT}} - 1} \quad (2\text{-}18)$$

By comparing both sides of the two equations, we find Einstein's relation

$$g_1 B_{21} = g_2 B_{12} \quad (2\text{-}29)$$

$$\frac{A_{21}}{B_{21}} = \frac{8\pi n^3 h\upsilon^3}{c^3} \quad (2\text{-}20)$$

Thus, at equilibrium, the population ratio between the two energy levels can be expressed using the Boltzmann law as follow:

$$\frac{N_2}{N_1} = \frac{g_2}{g_1} e^{-\frac{h\upsilon}{kT}} \quad (2\text{-}21)$$

Where:

g_i is the degeneracy of the energy level E_i,

T is the temperature,

k is Boltzmann's constant.

2.2.6. Optical amplification

Optical amplification refers to the process of enhancing the intensity of an optical signal through the use of different types of optical amplifiers. To enable laser operation, the active medium must be pumped using an external energy source. This pumping process excites the particles to higher energy states, establishing a condition known as population inversion, a non-equilibrium state in which more particles occupy excited states than ground states [7].

When these excited particles return to the ground state, they emit photons. A single photon can then stimulate another excited particle to emit a second photon that is identical in energy, phase, direction, and polarization a process called stimulated emission.

Through repeated occurrences of this process, optical amplification is achieved, as the number of coherent photons increases exponentially. This phenomenon forms the fundamental operating principal of the laser [7].

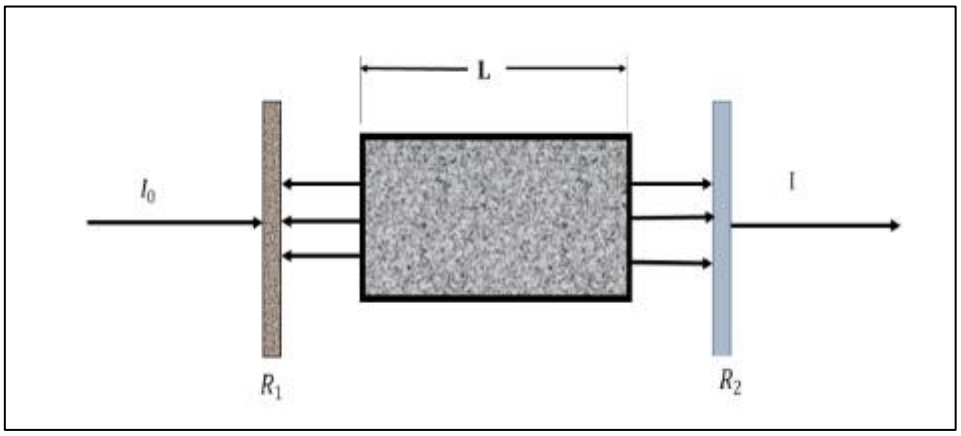

Figure (2-21): Illustrative diagram of the optical amplification process.

The losses in a laser system, excluding the output coupling loss through the partially transmitting front mirror can be described using a single comprehensive parameter known as the total loss coefficient, denoted by γ.

This coefficient is essential for determining the threshold condition for laser action, which is analysed by studying the variation in radiation intensity within the resonator over one complete round-trip. As the initial light beam propagates from the front mirror to the rear mirror inside the cavity, its intensity increases from I_0 to I, according to the following expression:

$$I = I_0 e^{(\gamma-\alpha)L} \qquad (2\text{-}22)$$

Where:

I_0 is the initial beam intensity,

I is the intensity after one round trip,

γ is the optical gain coefficient,

α is the total intracavity loss coefficient (excluding output coupling),

L is the length of the optical cavity.

When the optical beam is incident on the rear mirror, which has a reflectivity coefficient R_2 , the intensity of the reflected beam becomes:

$$I = I_0 R_2 e^{(\gamma-\alpha)L} \qquad (2\text{-}23)$$

After the optical beam reflects from the rear mirror and returns to be incident on the front mirror, which has a reflectivity R_1 , the beam completes a full round trip inside the resonator. At this stage, the final intensity of the light inside the cavity is give

$$I = I_0 R_1 R_2 e^{2(\gamma-\alpha)L} \quad (2\text{-}24)$$

The total gain in the laser system over one complete round trip in the resonator is expressed by the following equation:

$$G = \frac{I}{I_0} \quad (2\text{-}25)$$

$$G = R_1 R_2 e^{2(\gamma-\alpha)L} \quad (2\text{-}26)$$

If the total gain over one round trip in the resonator is greater than or equal to one ($G \geq 1$), the oscillation will be sustained within the optical cavity, allowing for the generation of a laser beam. However, if $G < 1$, the oscillation cannot be maintained, and the beam intensity will gradually decay, making laser emission impossible.

Thus, the condition $G = 1$ is regarded as the threshold condition that must be satisfied to initiate and sustain laser action.

$$G = R_1 R_2 e^{2(\gamma-\alpha)L} = 1 \quad (2\text{-}27)$$

$$\gamma_{th} = \alpha + \frac{1}{2L} \ln\left(\frac{1}{R_1 R_2}\right) \quad (2\text{-}28)$$

The first term of this equation represents the total losses in the system, while the second term represents the output. It is noted that the total gain over a complete cycle depends exponentially on the gain of the active medium, which in turn depends on the reflectance and type of active medium used.

2.3. Optical pumping

In a simple two-level system, it is not possible to obtain population inversion through optical pumping because absorption and stimulated emission occur with equal probability, preventing the accumulation of atoms in the excited state and thus inhibiting light amplification. Population inversion by optical pumping becomes possible when using a three-level system. Pump light with a shorter wavelength (higher photon energy) can transfer atoms from the ground state to the highest level. From there, spontaneous emission or a non-radiative process (involving phonons in a laser crystal) transfers atoms to an intermediate level, called the upper laser level. From that level down to the ground state, the laser transition with stimulated emission can occur. With sufficiently high pump intensity, population inversion for the laser transition can be reached as stimulated emission by the pump radiation is prevented by the transfer to the intermediate level [16].

Laser gain with a much lower excitation level is possible in a four-level system, such as Nd:YAG. Here, the lower level of the laser transition is somewhat above the ground state, and a rapid (most often non-radiative) transfer from there to the ground state keeps the population of the lower laser level very small. Therefore, a moderate population in the third level (the upper laser level), as achieved with a moderate pump intensity, is sufficient for laser amplification [19].

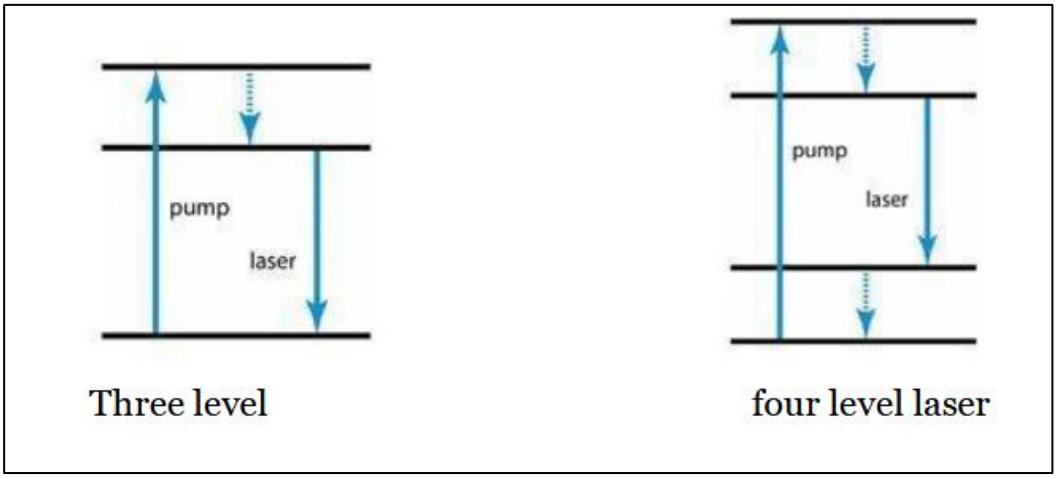

Figure (2-22): Optical Pumping: Three- and Four-Level Systems.

2.4. Types of lasers

Laser comes in different types depending on the material used to generate it.

2.4.1. Solid State lasers

Solid-state lasers are systems in which the active medium consists of solid crystals doped with active ions. These ions are typically transition metals or rare earth elements [14]. A typical solid-state laser includes the following components:

- **Active medium**

A solid crystal doped with laser-active ions that emit coherent light upon excitation. Common solid-state laser media include:

- ❖ Ruby
- ❖ Neodymium-doped Yttrium Aluminum Garnet (Nd:YAG)
- ❖ Neodymium-doped Glass (Nd:Glass)
- ❖ Alexandrite
- ❖ Titanium-doped Sapphire (Ti:sapphire)

Semiconductor lasers also fall under the solid-state category, although they differ by using semiconductor structures as the gain medium, which are pumped directly via electrical current rather than optical excitation [7].

- **Pumping source**

The most common pumping mechanism is the flashlamp, which emits intense light upon electrical excitation. This light is absorbed by the active medium, exciting the doped ions to higher energy states.

Alternatively, more efficient pumping methods include:

- ✓ Laser diode pumping
- ✓ Solar pumping, used in specialized applications

2.4.2. Gas lasers

Gas lasers utilize gaseous media such as: Helium (He) - Neon (Ne) - Carbon Dioxide (CO_2).

These lasers emit across a wide wavelength range, including ultraviolet (UV), visible, and infrared (IR) regions. A typical gas laser includes the following components:

- **Active medium**

A glass or ceramic discharge tube filled with:

✓ A single gas (argon, xenon, hydrogen, nitrogen);

✓ A gas mixture (helium-neon, hydrogen fluoride, xenon chloride);

✓ A multi-gas mixture (CO_2:He:N_2 lasers).

These gases cannot be optically pumped by flashlamps due to their narrow absorption spectra.

- **Pumping source**

An electrical power supply applies a voltage between two electrodes (anode and cathode) inside the tube, initiating a gas discharge that excites the atoms or molecules and produces laser emission.

2.4.3. Liquid-State lasers

liquid-State lasers also known as dye lasers, these lasers use organic dye solutions as the active medium and typically operate in the infrared region. They are highly tuneable and used in scientific research and medical applications [19]. A typical Liquid laser includes the following components:

- **Active medium**

An organic dye (Rhodamine) dissolved in a suitable solvent such as: Water – Ethanol - Other organic solvents

- **Pumping source**

Typically pumped using a flashlamp, similar to solid-state lasers. Alternatively, another laser (copper vapor laser) may be used for pumping, providing higher efficiency due to better spectral matching with the dye [14].

2.5. Nd:YAG laser

The Nd:YAG laser (Neodymium-doped Yttrium Aluminum Garnet, Nd^{3+}) is one of the most widely used solid-state lasers, owing to the unique characteristics of its crystal.

The Nd:YAG crystal exhibits the following characteristics [14,19]:

✓ High thermal conductivity

✓ Excellent optical quality

✓ A cubic crystalline structure, which enables:

- Narrow fluorescence linewidth;
- High optical gain
- Low lasing threshold

This laser operates as a four-level laser system, meaning four energy levels are involved in the lasing process. It typically emits in the near-infrared region, with a primary wavelength of 1064 nm, and may also emit at other wavelengths such as 940 nm, 1120 nm, 1320 nm, 1440 nm [20].

Nd:YAG lasers can operate in both continuous-wave (CW) and pulsed modes, making them highly suitable for various medical and scientific applications, including LASIK eye surgery and laser spectroscopy.

2.5.1. Structure of the Nd:YAG laser

The Nd:YAG laser consists of three essential components: a pumping source, an active medium (Nd:YAG crystal) and an optical resonator. In the active medium, yttrium ions $Y^{3+}$are partially substituted by neodymium ions Nd^{3+} within the YAG crystal lattice. The crystal is fabricated into a polished cylindrical rod with optically flat and parallel end faces to ensure efficient internal reflections. This laser rod is placed alongside the pumping source (usually a flashlamp) inside a highly reflective elliptical optical cavity, which enhances the laser emission [7].

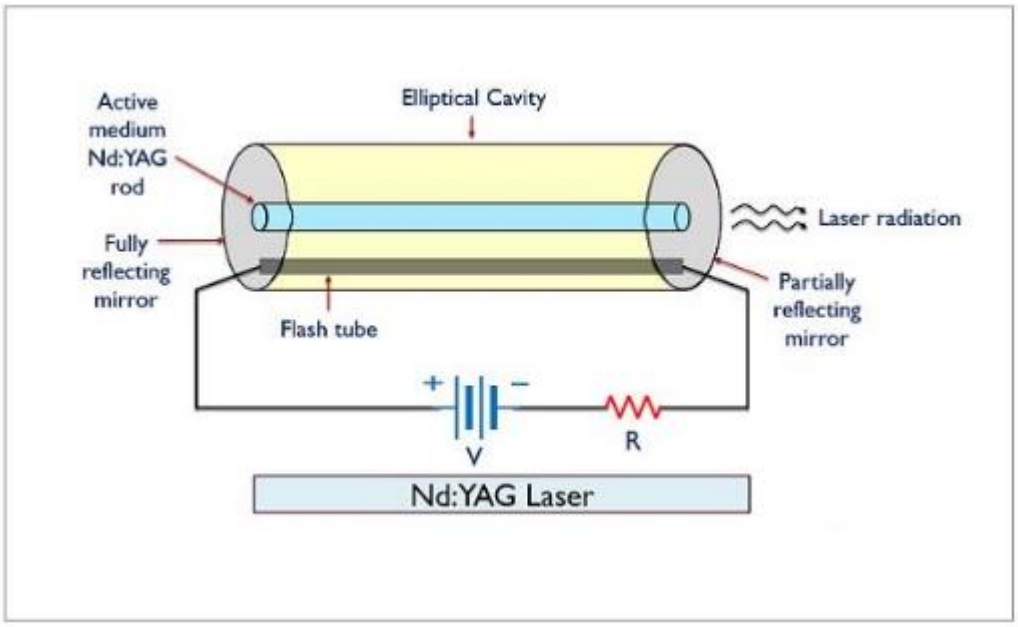

Figure (2-23): Structure of the Nd:YAG laser.

2.5.2. Operating principle of the Nd:YAG laser

Figure (2-7) illustrates the energy level diagram of Nd^{3+} ions within the Nd:YAG crystal, which governs the lasing mechanism [19][20].

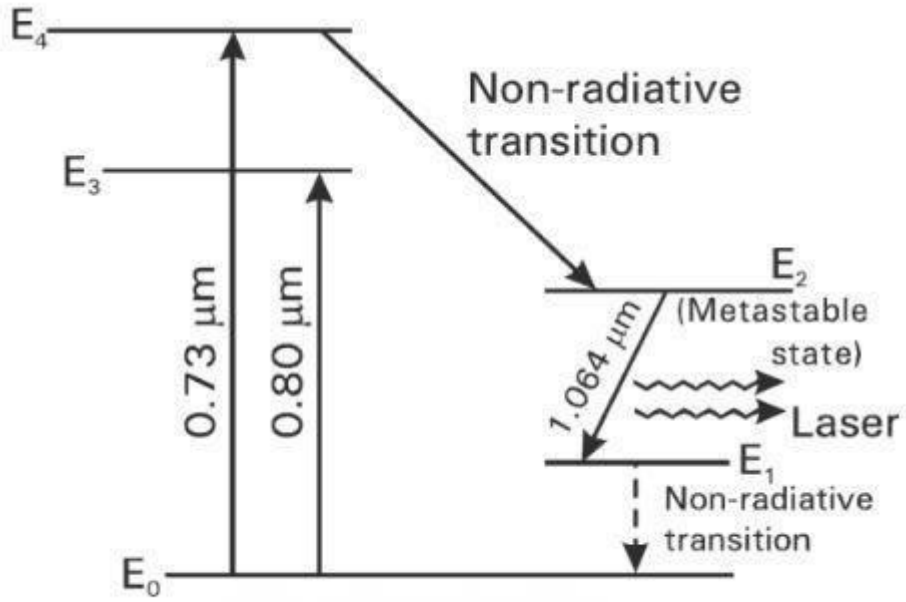

Figure (2-24) : energy level diagram.

2.5.3 Mechanism of operation

When the flashlamp is activated, it emits light that optically pumps Nd^{3+} ions from the ground state E_0 to higher energy states: to E_3 by absorbing photons with a wavelength of 0.80 µm and to E_4 by absorbing photons at 0.73 µm.

2.5.3.1 Internal relaxation:

The excited ions undergo non-radiative transitions from E_4 to the metastable level E_2through internal relaxation mechanisms (phonon interactions). Continuous excitation results in population inversion between levels $E_2$and E_1.

2.5.3.2 Laser emission:

Transition from E_2 to E_1 produces laser photons with a wavelength of 1064 nm. These photons stimulate additional emissions in phase and direction (stimulated emission). Photons traveling along the resonator axis undergo multiple reflections between mirrors, leading to amplification. Eventually, a portion of the light escapes through a partially reflective mirror, forming an intense, coherent laser beam [17,15].

2.5.3.3 Return to ground state:

The Nd^{3+}ions return to the ground state E_0 from E_1 via non-radiative transitions. Only a fraction of the flashlamp's energy is used for excitation; the remainder converts to heat. Thus, active cooling (air or water) is essential to maintain crystal integrity.

2.6. Solar laser technology

The solar laser system consists of several components that play a fundamental role in achieving the system's purpose. They can be basically classified into: the primary focusing system, the secondary focusing system, the cooling system, the tracking system, the laser medium (active medium), and the laser resonator or resonant cavity [19].

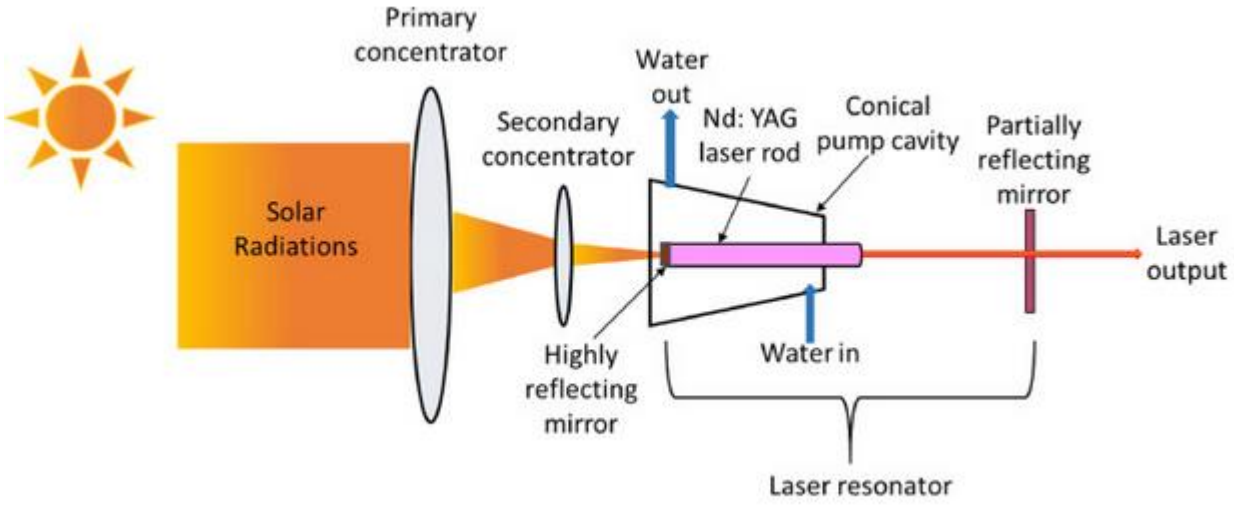

Figure (2-25): Schematic diagram of solar-powered solid-state Nd: YAG laser.

2.7. Solar laser pumping methods:

a-side-pumping

In side-pumping, concentrated sunlight is directed uniformly onto the cylindrical surface of the active medium (Nd:YAG laser rod). The light enters through the sidewalls of the crystal, allowing for a homogeneous distribution of pump light within the active medium [19].

This method offers several advantages:

Efficient and uniform energy deposition across the laser material.

Reduced thermal gradients, which contribute to better stability and enhanced laser performance [19,7].

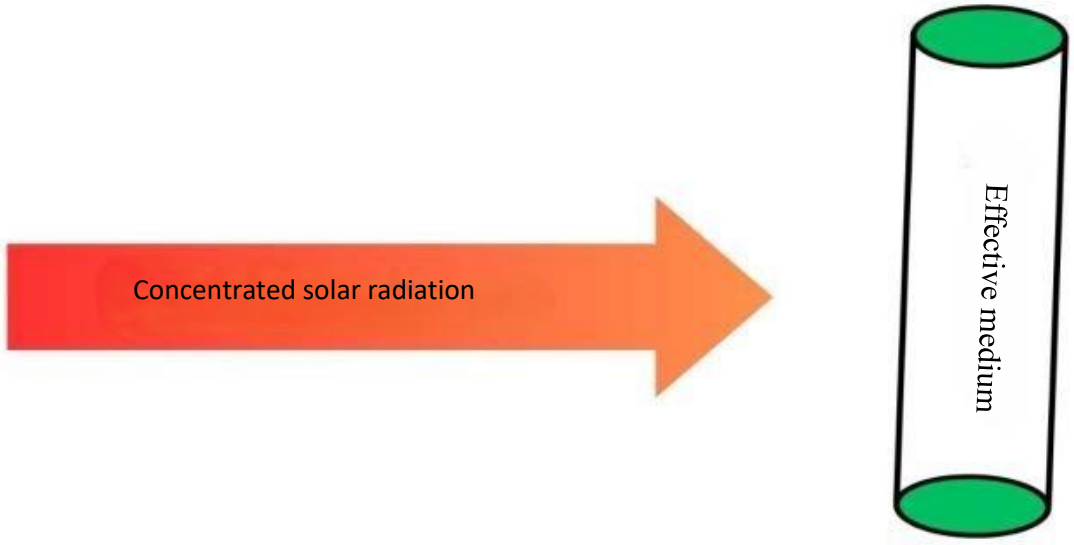

Figure (2-26): Side-pumping method.

b-End pumping:

In end-pumping, concentrated sunlight is directed into one end of the active medium, allowing the light to propagate longitudinally through the laser rod or crystal. This results in an uneven distribution of the pump light, with higher intensity near the input end and a gradual decline along the medium [19].

While this non-uniformity can be a disadvantage in some setups, end pumping is still beneficial in applications requiring:

High local pump intensity

Compact laser system designs

However, it necessitates careful thermal management to minimize thermal gradients and maintain stable laser output [19,7].

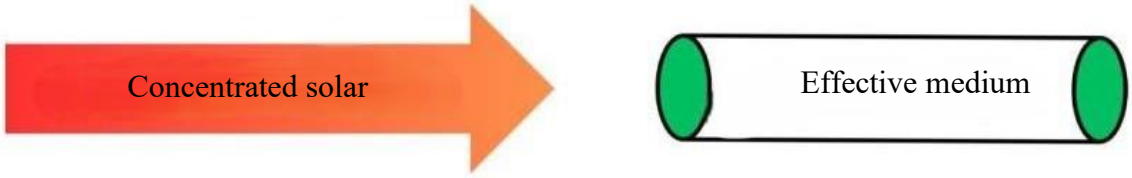

Figure (2-27): End-pumping method.

2.8. Energy conversion in a solar laser system

Energy conversion in a solar laser refers to the transfer of energy from solar radiation into a coherent laser beam. The performance of a solar-powered laser largely depends on both the overall system efficiency and the laser output power [13,14].

As previously discussed, a solar laser system is composed of multiple integrated optical and mechanical components, working together to convert sunlight into laser energy. Therefore, the design and optimization of these components play a critical role in determining the system's overall efficiency and output performance [17].

- ❖ Key factors affecting energy conversion efficiency include:
- ❖ The configuration and quality of the focusing optics (lenses and mirrors)
- ❖ The precision of the solar tracking system
- ❖ The spectral compatibility and performance of the active laser medium
- ❖ The cooling method employed to maintain thermal stability of the gain medium
- ❖ The threshold pump power p_{th} of a laser rod can be calculated using the following expression, which defines the minimum optical power required to initiate lasing in the active medium [7,17]:

$$P_{th} = \frac{A_\alpha I_s}{\eta_q \eta_{ovp} \alpha} \left(\frac{2\gamma_1 - \ln R}{2\varepsilon} \right) \quad (2\text{-}29)$$

Where:

A_α: The cross-sectional area of the rod.

I_s: The saturation flux.

η_q: The quantum efficiency.

η_{ovp}: The overlap ratio.

α: The absorption coefficient.

γ_1 : The losses in the rod.

ε: The pumping efficiency.

We can also calculate the slope efficiency value according to the following equation [17]:

$$\eta_s = \eta_q \eta_{ovp} \alpha \varepsilon \left(\frac{T}{2\gamma_1 - \ln R} \right) \quad (2\text{-}30)$$

Where: T is the permeability of the output coupler.

The laser output power can be written as follows

$$P_{out} = A_\alpha I_s \left[\frac{T}{2\gamma_1 - \ln R} \right] \left[g_0 - \left(\gamma_1 - \ln \sqrt{R} \right) \right] \quad (2\text{-}31)$$

where I_s is the saturation flux, T and R are the transmittance and reflectivity of the output mirror respectively, g_0 is the small signal gain; and γ_1 is the loss per crossing of the laser.

The laser output power can be written by the following equation

$$P_{out} = \eta_s \left(P_{in} - P_{th} \right) \quad (2\text{-}32)$$

2.9. Solar laser collection efficiency

The solar laser collection efficiency is defined as the ratio of the emitted laser power to the aperture area of the solar concentrator [7].

Its unit is: w^2/m

It can be expressed as:

$$\eta = \frac{P_{out}}{A_{ap}} \quad (2\text{-}33)$$

Where:

η is the collection efficiency of the solar laser.

P_{out}: is the laser output power.

A_{ap}:is the area of the solar center.

Conclusion

Point-focus solar concentrators, particularly parabolic dishes, are among the most effective systems for thermal energy conversion. They operate by concentrating solar radiation onto a thermal receiver located at the focal point, which absorbs the thermal energy and converts it into mechanical energy via a thermodynamic cycle.

In addition to their use in power generation, parabolic concentrators are also employed in laser production. A laser medium placed at the focal point absorbs the appropriate spectrum of solar radiation and emits laser light. This solar-pumped laser technology has wide-ranging applications in industry, medicine, and advanced technologies.

Chapter 3:

Numerical study, discussion and results

Chapter 3: Numerical study, discussion and results

3.1. Introduction

In this chapter, a numerical study is presented for a solar system designed to generate a solar-pumped laser using an Nd:YAG laser rod as the active medium. The study focuses on the lateral pumping of the laser rod by concentrated solar radiation collected using a parabolic dish concentrator with different dish radi R_{dish} and focal lengths f.

For each configuration, the total received solar radiation I is calculated, as well as the portion of radiation within the wavelength range[$\lambda_1 = 0.7\ \mu$m, $\lambda_2 = 300\ \mu$m].

The corresponding power associated with these radiation intensities is then determined.

Furthermore, the threshold power of the Nd:YAG active medium is evaluated using the parameters of the laser rod, including the rod cross-section area A_{rod} and the saturation irradiance I_S. The laser output power is then calculated considering the laser conversion efficiency η_{laser}.

Finally, the difference between the total collected radiation power and the power contained in the infrared spectral range considered in this study is analyzed.

The main objective of this chapter is to determine the intensity of concentrated solar radiation I_{focus} at the focal point of a parabolic solar dish for a specific day, and to analyze the influence of the dish radius R_{dish} and focal length f on both the concentrated intensity and the total collected energy.

3.2. Numerical modelling

- **Simplifying Assumptions of the model**

In our study, a set of parameters related to the solar resource has been defined. The period of study extends from sunrise to sunset.

In this paragraph, we consider a reflective system consisting of a solar reflector in the shape of a parabolic dish that focuses the incoming direct solar radiation onto a focal point.

This model has been simplified to suit the study conditions, based on the following assumptions:

1. Clear-sky conditions are assumed to ensure maximum solar irradiance.
2. Atmospheric effects, including absorption and scattering, are neglected, and the system is assumed to operate under ideal conditions.
3. The solar radiation is assumed to be uniform over the entire aperture area of the parabolic dish.
4. The reflectivity of the mirror is assumed constant over the entire surface and independent of wavelength.
5. Tracking errors are neglected, and the dish is assumed to be perfectly aligned with the sun throughout the day.

6. Optical losses due to surface imperfections, shading, and blocking effects are neglected.
7. The receiver is assumed to absorb all the concentrated radiation, with no reflection losses.
8. Thermal losses from the receiver (convection and radiation) are not considered in the optical concentration analysis.
9. The spectral filter is assumed ideal, transmitting only radiation within the selected wavelength range while completely blocking other wavelengths.

The study area is Ghardaïa Province, Algeria, chosen to evaluate the solar system performance according to the local solar radiation conditions. The geographical coordinates of the site are:

- Longitude Long=3.68333°
- Latitude φ=32.4833°
- Altitude Z=0.450 km above sea level.

The simulation considers different dish radii R_{dish}= [1.0,1.5,2.0]m and different focal lengths f= [0.6, 0.8, 1.0] m in order to evaluate the effect of the concentrator geometry on the collected solar energy and to generate a comparison table of the total concentrated energy for each configuration.

The simulation program is connected to:

- the geographical location,
- the selected date from the annual calendar (J, M),
- the solar incidence angle Θ.

The calculations are performed using a **MATLAB program**, together with several functions.

These functions take as inputs:

- I(t): hourly solar irradiance W/m2
- R_{dish}: dish radius (m)
- f: focal length (m)
- η_{opt}: optical efficiency of the system

and compute the following outputs:

- I_{focus}(t): concentrated solar intensity at the focal point (W/m^2)
- E_{total}: total daily collected energy (Wh)

Table 1: Main variables used in our program

Symbol	Value	Unit	Description
B	60	°	Dish inclination angle
J	21	—	Day of the month
M	12	—	Month (December)
Long	3.68333	°	Longitude of Ghardaia

Φ	32.4833	°	Latitude of Ghardaia
Z	0.450	km	Altitude above sea level
A_{atm}	0.88	—	Atmospheric transmittance coefficient
B_{atm}	0.26	—	Atmospheric attenuation coefficient
T_{min}	278	K	Minimum ambient temperature
T_{max}	298	K	Maximum ambient temperature
λ_1	0.7×10^{-6}	m	Minimum wavelength for IR spectrum
λ_2	300×10^{-6}	m	Maximum wavelength for IR spectrum
η_{focus}	0.9	—	Focusing system efficiency
R_{dish}	[1.0, 1.5, 2.0]	m	Array of dish radii used in simulation
f	[0.6, 0.8, 1.0]	m	Array of focal lengths used in simulation
P	0.8	—	Mirror reflectivity
T	0.2	—	Optical transmissivity
η_{opt}	0.75	—	Optical efficiency of the system
η_{lqser}	0.015	—	Laser conversion efficiency (YAG crystal)
A	0.6	—	Absorptivity of the active medium
A_{rod}	2.5×10^{-9}	m^2	Active laser rod cross-section area
I_S	1×10^{7}	W/m^2	Saturation irradiance
G_l	3	—	Geometric/loss factor
ε	0.8	—	Surface emissivity (used in heat transfer)
η_{cool}	0.05	°C/W	Cooling efficiency (temperature rise per watt)

The MATLAB program developed was based on the algorithm illustrated in the organigram present in figure (3-1). This algorithm models the optical and energetic performance of a parabolic solar concentrator over time. It begins by reading the input parameters such as dish geometry, geographic location, date, atmospheric conditions, and wavelength limits. Using these inputs, the algorithm computes key solar position parameters including solar declination, equation of time, solar time, hour angle, and solar height to determine whether the sun is above the horizon.

If solar radiation is available, the algorithm evaluates atmospheric effects by calculating air mass, beam irradiance, and tilted irradiance on the collector surface. It then iterates over the concentrator's geometric variables (radius and focal length) and over time steps. For each iteration, it determines the focused irradiance at the receiver, the input solar power, hourly collected energy, and the resulting output power. All computed values are stored and finally presented as tables and performance plots.

This iterative structure allows a detailed temporal and parametric analysis of the concentrator's efficiency and energy yield.

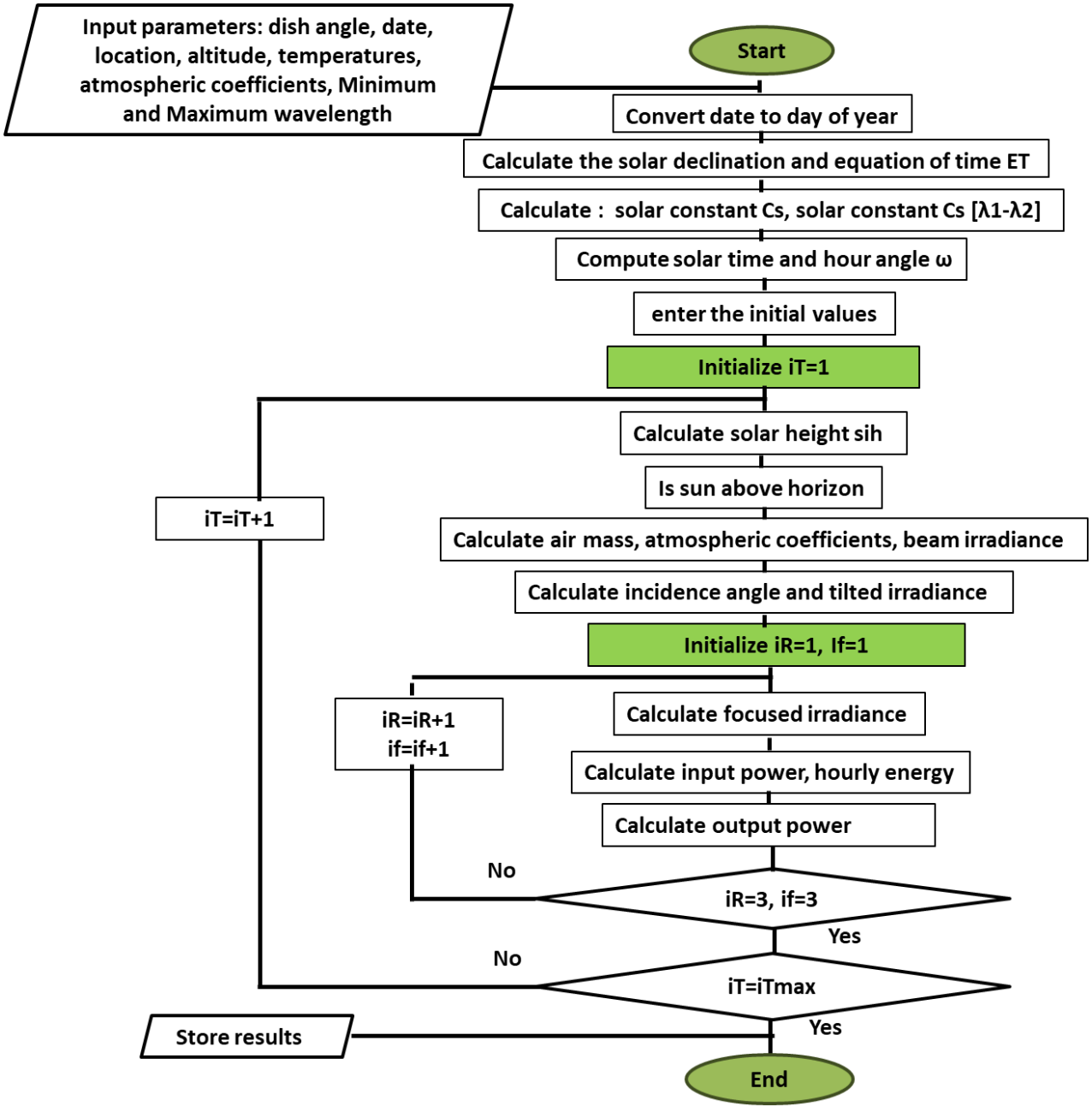

Figure (3-28): Flowchart of the optical and energy performance of a parabolic solar concentrator

3.3. Solar Irradiance

This graph represents the direct solar irradiance I in Ghardaïa on day J=355 of the year (December 21, near the winter solstice), assuming clear-sky conditions. It compares two irradiance curves as a function of time.

The solar constant G_{so} is taken as: G_{so}=1367 W/m2.

The integration is performed using numerical integration based on the Trapezoidal Rule over the wavelength range λ_1 =0.7µm - λ_2=300 µm in order to compute the solar radiation within this spectral interval.

The red curve represents the direct solar irradiance without spectral filtration. The direct irradiance as a function of time I(t) is calculated using equation (1–36).

The blue curve represents the solar irradiance after spectral filtration. A spectral filter that allows the transmission of electromagnetic waves within the wavelength interval $[\lambda_1, \lambda_2]$is considered.

The solar irradiance after filtration is calculated using the corresponding equations (equation (1-37), equation (1-38), equation (1-39) by integrating over the wavelength and multiplying by the solid angle of solar radiation.

The results show that the irradiance reaches its maximum around solar noon. The unfiltered irradiance reaches a peak value of approximately 850 W/m², while the irradiance after filtration reaches about 500 W/m².

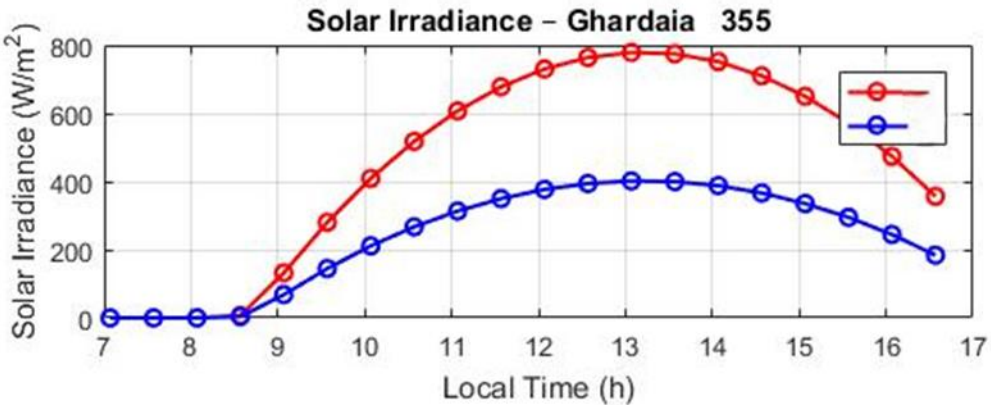

Figure (3- 29): The solar irradiance graph – Ghardaïa (day 355)

3.4. Optical behavior of a parabolic solar dish

This study investigates the behavior of a parabolic solar dish under varying dish radius (m) and focal length (m). The corresponding variations in the normalized focus radius (r_{focus}), the dish half-angle (ψ) expressed in radians, and the total collected energy (Wh) are analyzed.

- **Geometric parameters**

The geometric parameters significantly affect the performance of a parabolic solar dish.

The radius of point focus r_{focus} increases with focal length, since a longer focal length pushes the focus farther away.

ψ is the half-angle between the axis and the rim of the parabola, this angle calculated from the relation

$\psi = \tan^{-1}(\frac{2f}{R_{dish}})$

Where R_{dish} is dish radius and f is focal length

As the focal length increases, the angle ψ (narrower dish shape) decreases, and as the radius of the dish increases, the ψ (wider plate) increases as shown in the following table.

Table 2: Calculate values of ψ for different radii and focal lengths

R_{dish} (m)	f (m)	ψ (rad)
1.0	0.6	1.0304
1.0	1.0	0.7854
2.0	0.6	1.2793

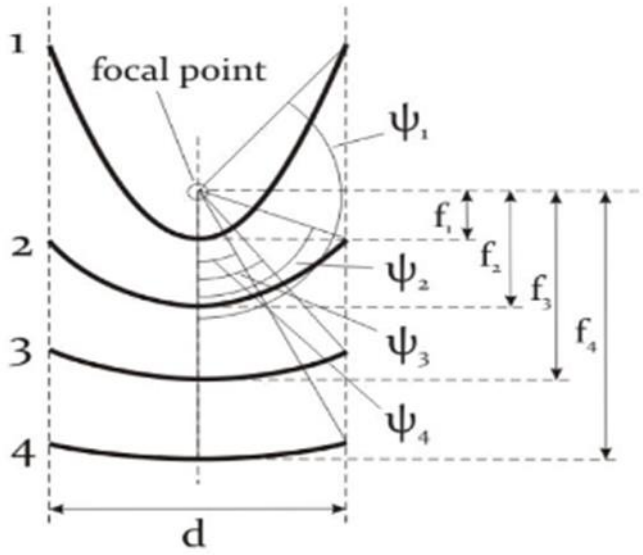

Figure (3-30): Focal length and ψ relation.

The normalized focus distance increases with longer focal lengths for a fixed dish radius. For example, in the case where the dish radius is 1 m:

- $f = 0.6 \rightarrow r_{focus} = 0.2956$
- $f = 1.0 \rightarrow r_{focus} = 0.3827$

A longer focal length shifts the focus point further from the center, increasing the relative focus distance.

3.5. Total energy collected (Wh)

The collected energy increases non-linearly with the size of the parabolic dish. This behavior is expected, as the dish surface area depends on the radius according to A=π $R_{dish}{}^2$. Consequently, the increase in energy collection is consistent with the growth of the reflective surface area. As the dish radius increases, the surface area grows quadratically, allowing the system to capture a larger amount of solar radiation and resulting in a significant increase in the energy output.

Table 3: Variation of focus radius, rim angle (ψ), and total energy with dish dimensions

R_{dish} (m)	f (m)	r_{focus}	ψ (rad)	E_{total} (Wh)
1.0	0.6	0.29562	1.0304	25,988
1.0	0.8	0.34655	0.89606	25,988
1.0	1.0	0.38268	0.7854	25,988
1.5	0.6	0.33638	1.1903	58,474
1.5	0.8	0.41160	1.0808	58,474
1.5	1.0	0.47186	0.98279	58,474
2.0	0.6	0.35816	1.2793	103,950
2.0	0.8	0.44850	1.1903	103,950
2.0	1.0	0.52573	1.1071	103,950

3.6. Total power collected

The power collected by the parabolic dish is determined using the theoretical expression given in equation (1–41). The effective collecting area of the dish (m²) is calculated from the radius R_{dish} of the aperture. The optical efficiency η_{opt}, defined within the range $0 < \eta_{\text{opt}} \leq 1$, accounts for optical losses in the system. In the present study, an efficiency value of $\eta_{\text{focus}} = 0.9$ is adopted.

Figures (3-4) and (3-5) present the time variation of the power collected by the dish. The parabolic dish has a radius $R_{dish} = 2$ m and a focal length $f = 1$ m.

The total power collected by the dish reaches a peak of about 8800 W around solar noon (1:30 p.m.). After filtering, the usable power drops to approximately 4500 W, meaning about 40-50% of the power is lost due to filtering and system inefficiencies.

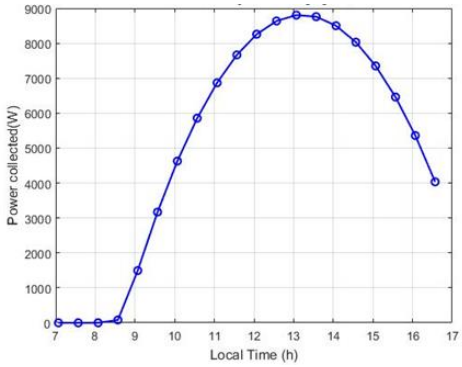

Figure (2-31): power collected [w]

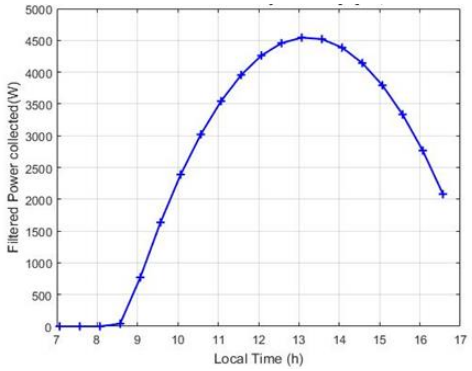

Figure (2-32): Filtered power collected [w].

3.7. Energy per hour

In this paragraph, we present the variation of energy per hour for the two cases:

The first figure illustrates the hourly collected energy [wh]. The energy output starts near zero around 7 – 8 a.m., then increases sharply from 9 a.m., reaching over 9,000 wh around 1 – 2 p.m., and finally decreases gradually until approximately 5 p.m.

The second figure represents the filtered energy per hour [wh]. This graph shows the filtered version of the energy data, with a clear trend of energy increasing from near zero at 9 a.m. to a peak around 1–2 p.m. (approximately 4,600 wh), followed by a gradual decrease.

The filtered data representation is considered the most appropriate option for long-term evaluation, system design planning, and supporting decision-making processes that rely on stable and highly reliable energy estimates.

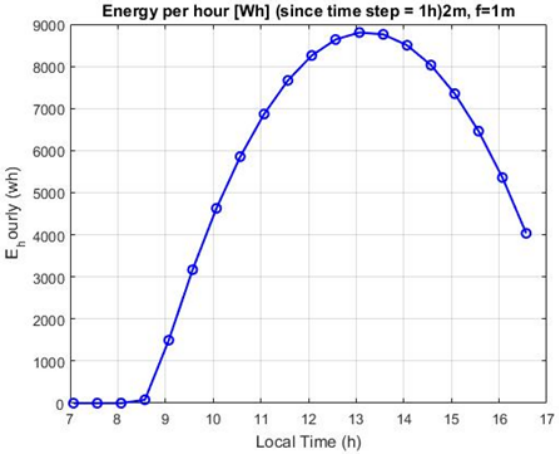

Figure (3-33): Energy per hour [wh].

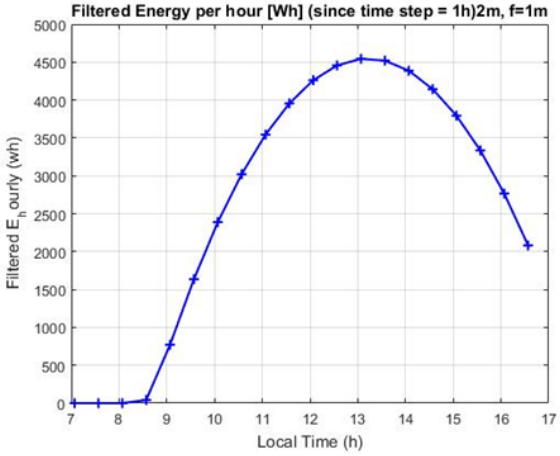

Figure (3-34): Filtered Energy per hour [wh].

3.8. Focused irradiance

The geometry of the parabolic dish is described by the parabolic equation ($z = r^2/4f$). This geometric configuration ensures that all incident solar rays parallel to the optical axis are reflected

toward the focal point. The aperture area of the dish is calculated using the following expression: ($A = \pi R_{dish}{}^2$), For a dish with a radius R_{dish}=2m, the aperture area is approximately: A≈12.57m².

The irradiance at the focal point depends on the concentration ratio C, defined in the equation (1-47). The focal irradiance can therefore be expressed as: I_{focus} = C×G×η_{opt} where G is the solar irradiance and η_{opt} represents the optical efficiency of the concentration system.

The total incident solar power received by the parabolic dish is determined by: P_{in} =G×A

Assuming an average solar irradiance G≈1000W/m², the total solar power intercepted by the dish is approximately P_{in}≈12570W

Case 1: Without Spectral Filter

In the first case, the entire solar spectrum is concentrated by the parabolic dish. The focal irradiance was calculated using the theoretical expression presented previously. The results are illustrated in Figure (3-8), which shows the variation of the focal irradiance as a function of the local time during the day.

As observed in the figure, the irradiance increases gradually from the morning hours, reaching a maximum value of approximately 10,000–10,500 W/m² around solar noon (about 13:00). After this peak, the irradiance decreases progressively during the afternoon. This behavior follows the daily variation of solar radiation intensity.

Case 2: With Spectral Filter

The spectral filter is assumed to transmit mainly infrared radiation within the wavelength range of approximately 0.7μm to 300μm, while blocking most of the ultraviolet and visible components of the solar spectrum. The spectral intensity of the direct solar radiation is calculated using the equation (1-38), then the power of the radiation concentrated on the solar receiver is calculated using the equation (1-42). The spectral intensity of the solar radiation transmitted to the receiver through the spectral filter in the range ($\lambda_1 \rightarrow \lambda_2$) is given by the equation (1-39). The focal irradiance in this configuration was calculated using the same theoretical expression.

The results shown in Figure (3-9) indicate that the peak focal irradiance decreases to approximately 5200–5300 W/m² near solar noon. This represents a reduction of nearly 50% compared with the case without the spectral filter. This decrease occurs because the filter transmits only a portion of the solar spectrum, mainly the infrared component.

Without a spectral filter,

We calculate the irradiance collected by the parabolic dish and foucus at the focal point using the theoretical expression given in equation (1–36). The results shown in the figure (3-8) when that the peak irradiance at the focal point reaches approximately 10 500 W/m².

With a filter that allows only thermal (infrared) radiation to pass through,

We calculate the irradiance in this case using the theoretical expression given in equation (1–39). The results shown in the figure (3-9). The peak irradiance in the filtered case decreases to about 5 300 W/m², indicating a reduction of nearly 50%.

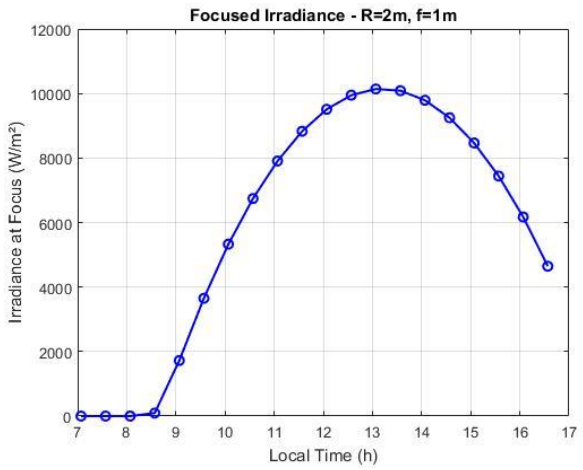

Figure (3-35): Focused irradiance without spectral filter R=2m, f=1m

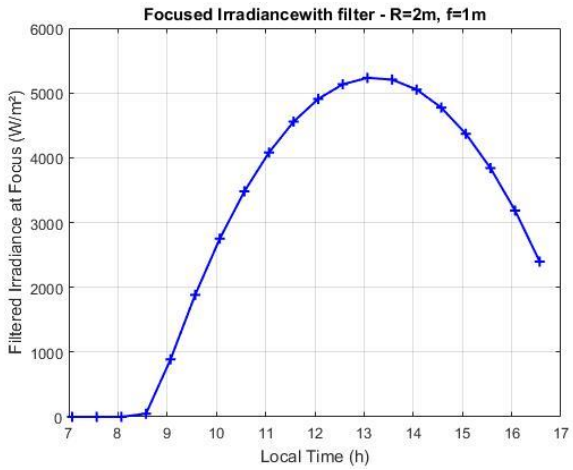

Figure (3-36): Focused irradiance with spectral filter R=2 m, **f** =1

3.9. Output laser with filter after conversion

The graph clearly demonstrates that the output laser power is highly dependent on solar irradiance throughout the day. The power output:

- Is zero or very low in the early morning (7– 9 a.m.) due to low solar angle.
- Increases sharply from 9 a.m. to 1 p.m., reaching a peak of ~52 W around 1:00 p.m., when the sun is highest.
- Gradually decreases in the afternoon as sunlight becomes less intense.

This pattern indicates that the system is solar-driven and performs best around solar noon. For improved performance, solar tracking, better conversion efficiency, and energy storage should be considered to extend useful operating hours.

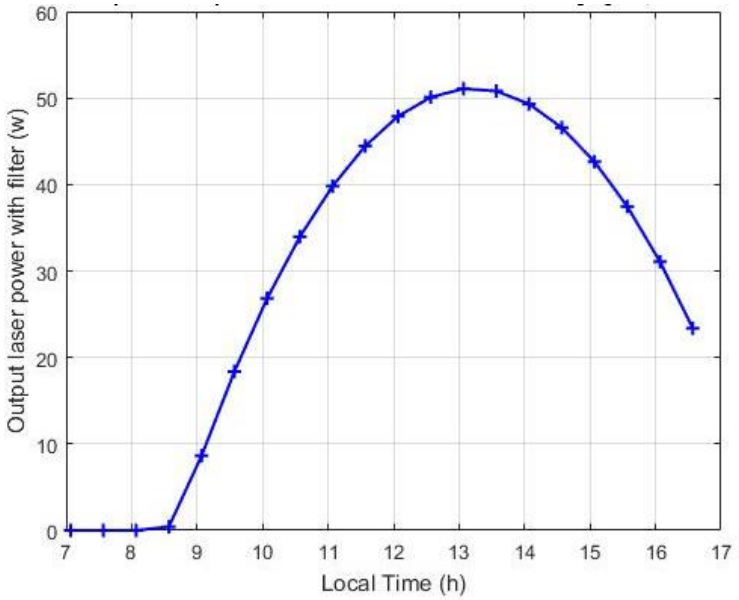

Figure (3-37): Output laser with filter after conversion [w] R=2 m, **f** =1 m.

Conclusion

Despite the decrease in total irradiance when using the filter, this is considered beneficial in applications that require a specific spectral range such as solar laser generation or high-efficiency thermal conversion systems where only the useful part of the solar spectrum (infrared radiation) is targeted. Filtering improves the quality of the concentrated energy and reduces losses caused by unwanted wavelengths.

Therefore, the use of spectral filters in solar concentration systems is recommended for thermal or optical applications that require precision and high efficiency, even if it leads to a reduction in total irradiance, as it enhances the overall performance and energy quality of the system.

General Conclusion

General conclusion

In conclusion, in light of current environmental challenges, particularly climate change and the continuous increase in fossil fuel consumption, renewable energy has emerged as a strategic option within global policies and a major field for scientific research and technological development. Among these sources, solar energy holds a prominent position due to its wide availability and versatility in both electrical generation and thermal applications.

Among the advanced applications of solar energy are solar radiation concentration systems, which rely on focusing sunlight using mirrors or lenses to achieve high energy densities and temperatures. This concentrated energy can be utilized to operate high-efficiency systems, including solar-pumped lasers based on active media such as Nd:YAG.

In this context, this study serves as an research step to analyze the performance of a solar-pumped Nd:YAG laser system based on a parabolic dish concentrator. By evaluating the behavior of concentrated solar radiation and its effectiveness in generating laser output power under different operating conditions—particularly the impact of spectral filtering—this work is considered a starting point for understanding the complex dynamics of solar-to-laser energy conversion.

The work is structured into three main chapters: the first examines solar radiation and concentrator physics; the second focuses on laser principles and solar pumping efficiencies; and the third provides a numerical analysis of the proposed system.

The results indicate that solar irradiance reaches its maximum around solar noon (about 850 W/m²), leading to high energy concentration at the focal point (up to 10,500 W/m² without filtering). The use of a spectral filter reduces both irradiance and collected energy by approximately 50%, with focal irradiance decreasing to about 5,300 W/m². Consequently, the collected power drops from about 8,800 W to around 4,500 W. As a result, the laser output power reaches a maximum of approximately 52 W around 1:00 PM.

These results provide preliminary confirmation that the parabolic dish concentrator is effective in focusing solar energy, while emphasizing that performance is highly dependent on optical and geometrical parameters. However, as a preliminary study, this work relies on numerical modeling under specific conditions without extensive empirical validation. Future research will focus on creating comprehensive models that take into account real-world climatic changes, conducting experimental validation, and exploring new active media materials to reduce thermal loss.

Ultimately, this work represents an introduction toward the study and development of efficient and sustainable solar-based technologies, advancing the horizons of solar energy applications and contributing to the transition toward clean energy innovation.

Références

REFERENCES

References

[1] U.S. Department of Energy, “Energy Efficiency and Renewable Energy,” DOE/GO-102001-1102, FS175, 2001.

[2] M. Ramero, D.Martinez, and E.Zarza,“Terrestrial solar thermal power plants: on the verge of commercialization”, in proceding of the 4th international conference on solar power from space, 2004.

[3] Soudani,M.E,et al., “experimental and theoretical study of parabolic trough collector (PTC) with a flat glass cover in the region of algerian sahara (Ouargla)” Journal of Mechanical Science and Technology,2017.31: p.4003-4009.

[4] Kelaus Jage,Olindo Isabella ,Arno H.M. Smets , Rene A.C.M.M .van Swaaij ,Mero Zeman , “Solar Energy Fundamentals,Technology, and systems copyright delft university of technology ,2014

[5] Duffie J. A., Beckman W. A., Solar Engineering of Thermal Process, Chapter 1, edited by John Wiley & Sons, Inc. 1991.

[6] D.Yogi Goswami ,Principal of solar engineering ,edited by Taylor & Francis Group,LLC .2015

[7] Aiadi Aicha,"Study of concentrated solar radiation for optoelectronic applications", Thèse of Doctorat, Université Kasdi Merbah Ouargla, 2023.

[8] S. Teske, L. Crespo and C. Richter, Solar thermal electricity,Global Outlook 2016, Greenpoace International, European SolarThermal Electricity Association ESTELA, Solar PACES ,2016.

[9] Anderson B. Solar energy: fundamentals in building design. New York: McGraw-Hill; 1977

[10] Kreider JF, Kreith F. Solar heating and cooling. New York:McGraw-Hill; 1977

[11] Saïd Mehellou, " Pompage optique des lasers par faisceau solaire", Thèse de Doctorat, Université Kasdi Merbah Ouargla, 2018.

[12] M. E. Soudani, F. Rehouma, K. E. Aiadi, Theoretical Study of a Glass-Covered Cylindrical Parabolic Solar Collector (CCP), Rev. sci. fond. app., vol. 2 N°. 1 (2010), 149-158

[13] Koechner W., Bass M., Solid State Lasers, Springer-Verlag Inc., New York, 2003.

[14] Liang, Dawei et Almeida, Joana.Highly efficient solar-pumped Nd:YAG laser .Optics. Express ,2011, vol.19, no 27, p. 26399-26405.

[15] Liang D., Almeida J., Solar-pumped TEM00 mode Nd:YAG laser. Opt. Express vol. 21, Issue 21, pp. 25107–25112, 2013.
https://doi.org/10.1364/OE.21.025107

[16] Abdel-Hadi, Yasser Abdel-Fattah. Development of optical concentrator systems for directly solar pumped laser systems. 2006.

[17] Dário Garcia, Dawei Liang, Cláudia R. Vistas, Hugo Costa, Miguel Catela , Bruno D. Tibúrcio and Joana Almeida, Ce:Nd:YAG Solar Laser with 4.5% Solar-to-Laser Conversion

REFERENCES

Efficiency, Energies,2022

[18] Dário Garcia, Dawei Liang, Cláudia R. Vistas, Hugo Costa,Bruno D. Tibúrcio, 32W TEM00-mode side-pumped solar laser design, Applied Solar Energy · December 2020.

[19] Daewook Kim, A review on design modalities of solar-pumped solid-state laser,Applied Surface ScienceAdvances,Volume12,2022,100348,ISSN,2666-5239, https://doi.org/10.1016/j.apsadv.2022.100348.

[20] Kato, T., Ito, H., Hasegawa, K., Ichikawa, T., Ikesue, A., Mizuno, S., Takeda, Y., Ichiki, A., Motohiro, T.: Energy transfer efficiency from Cr^{3+} to Nd^{3+} in Cr, Nd YAG ceramics laser media in a solar-pumped laser in operation outdoors. Opt. Mater. 110, 110481, 2020. https://doi.org/10.1016/j.optmat.2020.110481

[21] Cai, Z.; Zhao, C.; Zhao, Z.;Yao, X.; Zhang, H.; Zhang, Z. Highly Efficient Solar Laser Pumping Using a Solar Concentrator Combining a Fresnel Lens and Modified Parabolic Mirror. Energies 2022, 15, 1792. https://doi.org/10.3390/en15051792